Theory of the disordered $\nu = \frac{5}{2}$ quantum thermal Hall state: Emergent symmetry and phase diagram

Biao Lian[1] and Juven Wang[2]
[1]*Princeton Center for Theoretical Science, Princeton University, Princeton, New Jersey 08544, USA*
[2]*School of Natural Sciences, Institute for Advanced Study, Princeton, New Jersey 08540, USA*

(Received 30 January 2018; published 16 April 2018)

Fractional quantum Hall (FQH) system at Landau level filling fraction $\nu = 5/2$ has long been suggested to be non-Abelian, either Pfaffian (Pf) or antiPfaffian (APf) states by numerical studies, both with quantized Hall conductance $\sigma_{xy} = 5e^2/2h$. Thermal Hall conductances of the Pf and APf states are quantized at $\kappa_{xy} = 7/2$ and $\kappa_{xy} = 3/2$, respectively, in a proper unit. However, a recent experiment shows the thermal Hall conductance of $\nu = 5/2$ FQH state is $\kappa_{xy} = 5/2$. It has been speculated that the system contains random Pf and APf domains driven by disorders, and the neutral chiral Majorana modes on the domain walls may undergo a percolation transition to a $\kappa_{xy} = 5/2$ phase. In this paper, we do perturbative and nonperturbative analyses on the domain walls between Pf and APf. We show the domain wall theory possesses an emergent SO(4) symmetry at energy scales below a threshold Λ_1, which is lowered to an emergent $U(1) \times U(1)$ symmetry at energy scales between Λ_1 and a higher value Λ_2, and is finally lowered to the composite fermion parity symmetry $\mathbb{Z}_2^F$ above Λ_2. Based on the emergent symmetries, we propose a phase diagram of the disordered $\nu = 5/2$ FQH system and show that a $\kappa_{xy} = 5/2$ phase arises at disorder energy scales $\Lambda > \Lambda_1$. Furthermore, we show the gapped double-semion sector of N_D compact domain walls contributes nonlocal topological degeneracy 2^{N_D-1}, causing a low-temperature peak in the heat capacity. We implement a nonperturbative method to bootstrap generic topological $1+1$D domain walls (two-surface defects) applicable to any $2+1$D non-Abelian topological order. We also identify potentially relevant spin topological quantum field theories (TQFTs) for various $\nu = 5/2$ FQH states in terms of fermionic version of $U(1)_{\pm 8}$ Chern-Simons theory $\times\, \mathbb{Z}_8$-class TQFTs.

DOI: 10.1103/PhysRevB.97.165124

I. INTRODUCTION

The filling fraction $\nu = 5/2$ fractional quantum Hall (FQH) state in $2+1$ dimensional ($2+1$D) spacetime is one of the few non-Abelian state candidates which show experimental evidences [1]. Exact diagonalization (ED) and density matrix renormalization group (DMRG) studies in the past [2–11] have shown the $\nu = 5/2$ ground state favors either the Moore-Read Pfaffian (Pf) state [12,13] or its particle-hole (PH) conjugate, the anti-Pfaffian (APf) state [14,15], both of which are non-Abelian. (See also an early theoretical work on non-Abelian states [16].) More precisely, the ground state is found to be either the Pf state or the APf state at half filling in the spin polarized first Landau level, together with two fully occupied spin up and down zeroth Landau levels. While both states exhibit a quantized Hall conductance $\sigma_{xy} = 5/2$ in units of e^2/h where e is the electron charge and h is the Planck constant, the thermal Hall conductance κ_{xy} of the Pf state and the APf state are quantized differently at $\kappa_{xy} = 7/2$ and $\kappa_{xy} = 3/2$ in units of $\pi^2 k_B^2 T/3h$, respectively, where k_B is the Boltzmann constant and T is the temperature. Theoretically, κ_{xy} is the total chiral central charge of the $1+1$D edge conformal field theory (CFT) of a bulk-gapped $2+1$D topological state [17] (Appendix A). For Pf and APf states, the half-integer κ_{xy} is due to the existence of an odd number of neutral chiral Majorana-Weyl fermions on the edge [18] in addition to charged chiral bosons (or complex fermions).

Recently, a measurement by Banerjee *et al.* [19] observed that the thermal Hall conductance of the $\nu = 5/2$ FQH state is $\kappa_{xy} = 5/2$, which is in contradiction to both the Pf state and the APf state. Instead, this experimental result [19] agrees with a different non-Abelian state candidate known as the particle-hole Pfaffian (PH-Pf) state [20–22] (Appendix A). However, it is generically believed the PH-Pf state is not energetically favored compared to the Pf or APf state, with evidences from numerical calculations (see discussion in Ref. [23]). Most recently, it is suggested that the presence of disorders may stabilize the PH-Pf state, and various other possible phases under disorders are discussed [23,24]. The idea is that the disorders may drive the $2+1$D system into random domains of Pf and APf states (Fig. 1), where each domain wall carries chiral central charge $c_- \equiv c_L - c_R = 2$ and hosts four chiral Majorana edge states. The percolation of these chiral Majorana edge states in the bulk of the system may then yield different phases in the infinite size thermodynamic limit, including a possible $\kappa_{xy} = 5/2$ phase which is identified with the PH-Pf state. However, several problems still remain unsettled, which include a detailed analysis of the edge theory on the domain walls, emergent symmetries at low energies, the disorder strength for the $\kappa_{xy} = 5/2$ phase to be stabilized, and the energy cost of domain walls in the system, etc.

In this paper, we study the edge theory and possible emergent symmetries on the domain wall between Pf and APf states, based on which, we propose a possible yet more specific phase diagram of the disordered system. We show the effective theory of the domain wall has an emergent SO(4) symmetry at low energies below an energy scale Λ_1, which breaks down

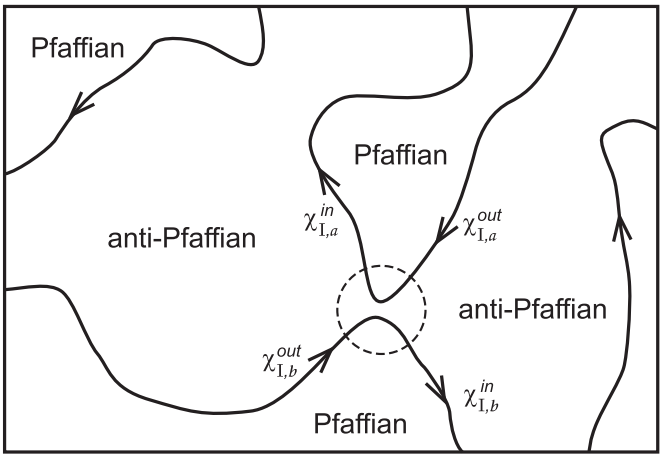

FIG. 1. Random domains of Pfaffian and anti-Pfaffian states with percolating domain walls, where each domain wall possesses four chiral Majorana fermion modes along the direction of the arrow. When two domain walls get close to each other as shown by the dashed circle, the chiral Majorana fermions on them may tunnel between them.

to a $U(1) \times U(1)$ emergent symmetry at intermediate energy scales between Λ_1 and Λ_2, and finally to a fermion parity $\mathbb{Z}_2^F$ symmetry at energy scales above Λ_2. This leads to our phase diagram in the vicinity of $\nu = 5/2$ as shown in Fig. 2, where ν is the filling fraction, and Λ is the disorder strength. In the absence of disorders, as shown by previous numerical studies [2–11], the ground state is the Pf state (with quasiholes) for $\nu < \nu_c$ and is the APf state (with quasielectrons) for $\nu > \nu_c$, where $\nu_c \approx 5/2$ is the critical filling fraction. When the energy scale of disorders $\Lambda < \Lambda_1$ is weak, there is just a single transition from Pf to APf phase with respect to ν as ensured by the emergent SO(4) symmetry. At intermediate disorder energy scales $\Lambda_1 < \Lambda < \Lambda_2$, the emergent symmetry is lowered to $U(1) \times U(1)$, and the single transition with respect to ν splits into two transitions, with a new gapped phase of $\kappa_{xy} = 5/2$

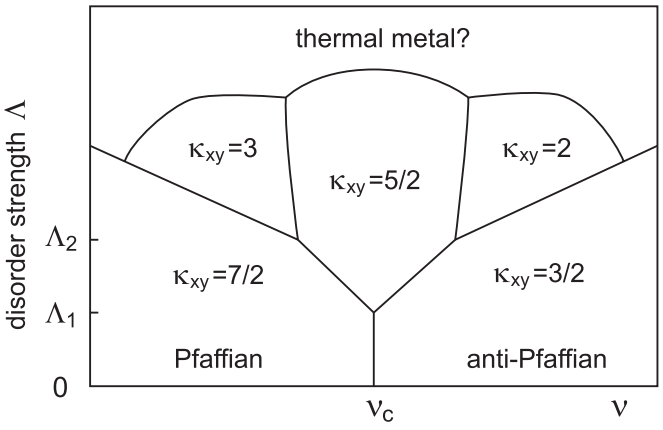

FIG. 2. We propose the specific phase diagram of disordered $\nu = 5/2$ state, where ν is the mean filling fraction, Λ is the disorder energy scale inversely proportional to Pf or APf domain size, and the phases are labeled by thermal Hall conductance κ_{xy}. The system exhibits an SO(4) emergent symmetry for $\Lambda < \Lambda_1$ and has a $U(1) \times U(1)$ emergent symmetry for $\Lambda_1 < \Lambda < \Lambda_2$.

arising between the Pf and APf phases. Here the disorder energy scale Λ is roughly inversely proportional to the size of a Pf or APf domain. For higher disorder energy scales $\Lambda > \Lambda_2$ where only $\mathbb{Z}_2^F$ symmetry remains, the system may undergo four phase transitions with respect to ν, each of which changes κ_{xy} by $1/2$, or the system may enter a thermal metal phase where the bulk becomes gapless [25–27]. We note that since emergent symmetries are not "true" exact symmetries, it is possible the above picture is only approximately true, namely, the single phase transition at $\Lambda < \Lambda_1$, and two phase transitions at $\Lambda_1 < \Lambda < \Lambda_2$ with respect to ν may be broadened and are not sharp transitions. Such broadenings are, however, expected to be at least exponentially suppressed by factors $e^{-\Lambda_1^2/\Lambda^2}$ and $e^{-\Lambda_2^2/\Lambda^2}$ [23,28,29], respectively, and are probably beyond the resolution of the experiments. Nevertheless, it is still possible that there are no broadenings at all due to dynamical fluctuations, and all phase transitions in the phase diagram Fig. 2 are sharp, which calls for a future study. Finally, we show that the charged sector of the domain walls, although being gapped out, also has a nontrivial contribution to the nonlocal topological ground state degeneracy [30,31], which affects the heat capacity and longitudinal thermal conductance of the system.

We first briefly review the topological properties of the Pf and APf states. In the original work by Moore and Read [12], the Pf state is a filling fraction $\nu = 1/2$ wave function in the zeroth Landau level

$$\Psi_{\rm Pf} = \prod_{1=i<j}^{N} (z_i - z_j)^2 {\rm Pf}\left(\frac{1}{z_i - z_j}\right) \prod_{i=1}^{N} e^{-|z_i|^2/4\ell_B^2}, \quad (1)$$

where N is the number of electrons which is even, $\ell_B = \sqrt{\hbar c/eB}$ is the magnetic length of magnetic field B, $z_i = x_i + iy_i$ is the complex coordinate of the ith electron, Pf gives the Pfaffian of the antisymmetric matrix $M_{ij} = 1/(z_i - z_j)$, and all the electrons are spin polarized. In the context here, both the spin up and down in the zeroth Landau levels are fully occupied, and the Pf state is formed in the spin polarized first Landau level, so the total filling fraction is around $\nu = 5/2$. The gapped bulk of the Pf state allows the existence of both charge $\pm e/2$ semions which are Abelian and charge $\pm e/4$ quasiparticles which obey non-Abelian statistics [32]. The gapless edge of the Pf state contains a left-moving charge $e/2$ chiral boson mode and a left-moving neutral chiral Majorana fermion mode [33]. Together with two left-moving charge e chiral complex fermion modes from the spin up and down zeroth Landau levels, they contribute a Hall conductance $\sigma_{xy} = 5/2$ and a thermal Hall conductance $\kappa_{xy} = 7/2$.

The APf state is obtained by applying a particle-hole transformation [34] to the Pf state in the first Landau level. The edge theory of the APf state consists of a left-moving charge e chiral complex fermion, a right-moving charge $e/2$ chiral boson, and a right-moving neutral chiral Majorana fermion. Under disorders, such an edge theory renormalizes into a charge $e/2$ left moving chiral boson, and an SO(3) symmetric triplet of right-moving neutral chiral Majorana fermions therefore develops an SO(3) emergent symmetry [14,15]. At $\nu = 5/2$, this yields a Hall conductance $\sigma_{xy} = 5/2$ and a thermal conductance $\kappa_{xy} = 3/2$. Meanwhile, the bulk

of APf state also hosts charge $\pm e/2$ semions and charge $\pm e/4$ non-Abelian quasiparticles, but slightly different from those in the bulk of Pf state. Using the above information, we identify the detailed bulk topological quantum field theories (TQFTs) and gapless edge theories (conformal field theories coupling to external background fields) of Pf, APf, PH-Pf states and other related $\nu = 5/2$ states, which can be found in Appendix A.

A useful perspective often adopted in literature is to view the Pf and APf states as superconductors of composite fermions with different pairing symmetries [13,21,35]. A composite fermion is defined as an electron bound with two statistical gauge field fluxes, which cancel the external magnetic field on average for a half-filled Landau level [21,35,36]. It is believed to be a good starting point to assume the composite fermions in the first Landau level form a Fermi liquid with a single Fermi surface [21,37]. Recent studies suggest the Fermi liquid may be a Dirac Fermi liquid, and the Fermi surface has an intrinsic π Berry phase [21,37–41]. The Fermi surface can then be gapped out by forming Cooper pairs. If we denote the composite fermion at momentum $\mathbf{k}$ as $f_{\mathbf{k}}$, the possible pairing amplitude $\Delta(\mathbf{k}) f_{\mathbf{k}} f_{-\mathbf{k}}$ near the Fermi surface must satisfy $\Delta(\mathbf{k}) = -\Delta(-\mathbf{k})$ because of the anticommutation relation of $f_{\mathbf{k}}$ and $f_{-\mathbf{k}}$. Namely, the pairing must have an odd parity. In particular, a $p + ip$ pairing amplitude $\Delta(\mathbf{k}) = \Delta_{\mathrm{Pf}} e^{i\theta_{\mathbf{k}}}$ near the Fermi surface leads to the Pf state, while a $f - if$ pairing amplitude $\Delta(\mathbf{k}) = \Delta_{\mathrm{APf}} e^{-3i\theta_{\mathbf{k}}}$ corresponds to the APf state, where $\theta_{\mathbf{k}} = \arg(k_x + ik_y)$ is the polar angle of the momentum [13,21].[1] This picture correctly reproduces the neutral sector of edge theories of the Pf and APf states, i.e., a left-moving chiral Majorana mode on the Pf state edge and three right-moving chiral Majorana modes on the APf state edge. Besides, the PH-Pf state corresponds to a $p - ip$ pairing $\Delta(\mathbf{k}) = \Delta_{\mathrm{PH}} e^{-i\theta_{\mathbf{k}}}$ of the Fermi surface [20,21], although this state may be energetically unfavored. We note that, however, the above pairing picture cannot reproduce the charged sector, namely, the $e/2$ left-moving chiral boson mode on the edges of Pf, APf, and PH-Pf states.

In the presence of chemical potential disorders, the local filling fraction $\nu(\mathbf{r})$ may vary spatially above and below ν_c, and the system may be driven into random domains of Pf and APf states as shown in Fig. 1. The domain wall between Pf and APf states carries a chiral central charge $c_- = 2$, and it is easy to see from the above pairing picture that there are four neutral chiral Majorana fermion modes of the same chirality on the domain wall. The system is then a random percolation system of chiral Majorana fermions. When two domain walls are close to each other as shown by the dashed circle in Fig. 1, the chiral Majorana fermions χ_I $(1 \leqslant I \leqslant 4)$ on them may tunnel into each other. Such a tunneling can be generically expressed as $\chi^{\mathrm{out}}_{I,\tau} = (O^{\mathrm{out},\tau}_{IJ} S^J_{\tau\tau'} O^{\mathrm{in},\tau'}_{JI'}) \chi^{\mathrm{in}}_{I',\tau'}$, where $\chi^{\mathrm{in/out}}_{I,\tau}$ ($\tau = a,b$ is the domain wall label) are in/out chiral Majorana modes around the dashed circle as shown in Fig. 1, $O^{\mathrm{in},\tau}$ and $O^{\mathrm{out},\tau}$ are random SO(4) rotation matrices mixing the four Majorana modes of a domain wall and obeying a certain distribution (e.g., Gaussian), and $S^I_{\tau\tau'}$ are the 2×2 scattering matrices defined by

$$S^I = \begin{pmatrix} \cos\alpha_I & \sin\alpha_I \\ -\sin\alpha_I & \cos\alpha_I \end{pmatrix}, \tag{2}$$

where α_I $(1 \leqslant I \leqslant 4)$ are usually called scattering angles. In addition, due to disorder, the four chiral Majorana modes on the same domain wall may be mixed and thus propagate into each other. In addition, the propagation of chiral Majorana fermions χ_I on domain wall τ may also involve a flavor mixing due to disorders, namely, $\chi_{I,\tau}(x') = O^{\tau}_{IJ}(x',x)\chi_{J,\tau}(x)$, where the propagation matrix $O^{\tau}(x,x')$ is a random SO(4) matrix obeying certain distributions, while x and x' denote the 1D coordinate of the domain wall. Such a percolation system can be studied numerically using random network models [23,24,42,43]. In particular, if none of the angles α_I are equal, the system belongs to the D symmetry class (with only a fermion parity $\mathbb{Z}_2^F$ symmetry) and is the least symmetric [43,44].

The spatial mean values $\langle\alpha_I\rangle$ of α_I $(1 \leqslant I \leqslant 4)$ are monotonic functions of the average filling fraction ν. When ν is far above (below) ν_c, the system is in the APf (Pf) state, and all the $\langle\alpha_I\rangle$ tend to 0 ($\pi/2$). When one increases ν from far below ν_c, whenever an $\langle\alpha_I\rangle$ becomes equal to $\pi/4$, a chiral Majorana fermion mode will be delocalized in the bulk and extend to the edge between the system and the vacuum, which is the percolation transition point. After $\langle\alpha_I\rangle$ has passed by $\pi/4$, a chiral Majorana edge state on the edge of the system will be eliminated or created, and the chiral central charge on the edge of the system will change by $1/2$. Figure 3 shows an example how a chiral Majorana edge state is eliminated (created) after the percolation transition of a chiral Majorana mode in the bulk. Therefore, if the system is in the D symmetry class, one expects four phase transitions with respect to ν for disorders not too strong (which potentially causes thermal metal), during which κ_{xy} undergoes four transitions from $7/2 \to 3 \to 5/2 \to 2 \to 3/2$ [23,24]. For strong disorders especially those coming from random π flux vortices, the system may enter a gapless thermal metal phase where κ_{xy} is no longer quantized [25–27].

There is, however, a possibility that the domain walls between Pf and APf states possess certain emergent symmetries, which enforce two or more α_I angles to be equal everywhere. In this case, the system will undergo less phase transitions with respect to ν. For instance, if the four chiral Majorana fermions on the domain wall possess an SO(4) rotational symmetry during scattering, all the four scattering angles α_I will be equal, and one would expect a single phase transition directly from the Pf state to the APf state. Such emergent symmetries may generically arise from interactions and disorders [45,46]. For instance, an SO(3) symmetry emerges on the edge of APf state due to disorder [14,15]. The following sections are devoted to explore the possibility of emergent symmetries and how the phase diagram will be modified.

[1] In the literature of Dirac Fermi liquid, the Fermi surface π Berry phase is embedded in the definition of $f_{\mathbf{k}}$, namely, $f_{\mathbf{k}} \to e^{i\theta_{\mathbf{k}}/2} f_{\mathbf{k}}$, so the $p + ip$-pairing Pf state, $p - ip$-pairing PH-Pf state, and $f - if$-pairing APf state are denoted as $d + id$, s, and $d - id$ pairing, respectively. This is just a different definition of basis and does not change any physics. To be precise, by s, $p \pm ip$, $d \pm id$, and $f \pm if$ pairings we mean $\Delta(\mathbf{k}) \propto 1$, $k_x \pm ik_y$, $(k_x \pm ik_y)^2$, and $(k_x \pm ik_y)^3$, respectively. See also discussions in Appendix A.

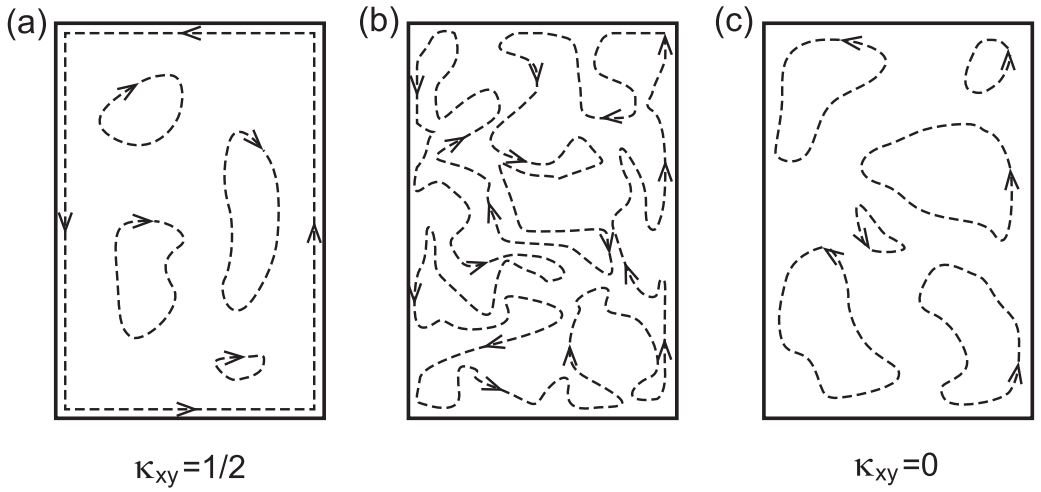

FIG. 3. Illustration of the percolation transition of a single chiral Majorana fermion mode, which is represented by the dashed line with arrows indicating the chirality. (a) Before the percolation transition, where all the bulk chiral Majorana states are localized, there is a chiral Majorana edge state on the edge contributing $\kappa_{xy} = 1/2$. (b) At percolation transition point, the bulk chiral Majorana mode is delocalized and connects with the edge state randomly. (c) After the percolation transition, the original edge state breaks up into localized states, and the thermal Hall conductance becomes $\kappa_{xy} = 0$. To make an analogy, in Fig. 1, the Pf-APf forms an archipelago-sea relation. When the sea level (filling-fraction ν) decreases ($\nu < \nu_c$ in Fig. 2), the land (Pf) delocalizes and the sea (APf) localizes. When the sea level increases ($\nu > \nu_c$ in Fig. 2), the land (Pf) localizes and the sea (APf) delocalizes. At the transition ($\nu \simeq \nu_c$ in Fig. 2), both the land (Pf) and sea (APf) delocalize, which means the domain walls also delocalize, percolating to the boundary (of the experimental sample).

II. EXAMPLE OF DISORDERED SUPERCONDUCTOR WITH EMERGENT $U(1)$ SYMMETRY

Before we proceed to the $\nu = 5/2$ FQH system, it is useful to study a simpler but similar $2+1$D system of random $p+ip$ and $p-ip$ superconducting domains, which we shall show has an emergent $U(1)$ symmetry. Importantly, we assume the system before superconducting has a single Fermi surface, described by Hamiltonian

$$H_0 = \sum_{\mathbf{k}} \left(\frac{k^2}{2m_0} - \mu \right) c^\dagger_{\mathbf{k}} c_{\mathbf{k}}, \tag{3}$$

where $c_{\mathbf{k}}$, $c^\dagger_{\mathbf{k}}$ are the electron annihilation and creation operators with $\mathbf{k}$ being momentum, $\mu > 0$ is the chemical potential, $m_0 > 0$ is the effective electron mass, and we have set the Plank constant $\hbar = 1$. The single Fermi surface requires the parity of the pairing amplitude $\Delta(\mathbf{k})$ to be odd. Here we assume the pairing depends on an interaction parameter λ, so that the system prefers a $p+ip$ pairing $\Delta(\mathbf{k}) = \Delta_+ e^{i\theta_{\mathbf{k}}}$ for $\lambda > 0$, and prefers a $p-ip$ pairing $\Delta(\mathbf{k}) = \Delta_- e^{-i\theta_{\mathbf{k}}}$ for $\lambda < 0$, with $\theta_{\mathbf{k}} = \arg(k_x + ik_y)$. Accordingly, the clean system is a chiral topological superconductor with a left-moving (right-moving) chiral Majorana fermion on the edge when $\lambda > 0$ ($\lambda < 0$) [13] and has a thermal Hall conductance $\kappa_{xy} = 1/2$ ($\kappa_{xy} = -1/2$). As long as the chemical potential $\mu > 0$, there will be no trivial superconductor phase in between, and only a single phase transition exists between the $p \pm ip$ superconductor phases with respect to λ.

In the presence of disorders, λ may have a spatial fluctuation, and random domains of $p+ip$ and $p-ip$ superconductivity will occur when the spatial mean value $\langle\lambda\rangle$ is near 0. Each domain wall has two chiral Majorana fermions of the same chirality. If there is no additional symmetry, the system is in the D symmetry class, and the system should exhibit two delocalization phase transitions with respect to $\langle\lambda\rangle$, with κ_{xy} changing from $1/2 \to 0 \to -1/2$. However, one expects the $\kappa_{xy} = 0$ phase to vanish for sufficiently weak disorders (when the Fermi surface picture is still valid), since such a gapped phase does not correspond to any pairing of a single Fermi surface. It is therefore more natural to expect the $\kappa_{xy} = 0$ phase does not occur until the disorder strength reaches a certain threshold.

We shall show this is ensured by an emergent $U(1)$ symmetry on the domain walls at low energies. The pairing amplitude near a domain wall can be generically written as

$$\Delta(\mathbf{k}) = \Delta_+(\mathbf{r}) e^{i\theta_{\mathbf{k}}} + \Delta_-(\mathbf{r}) e^{-i\theta_{\mathbf{k}}}, \tag{4}$$

where $\Delta_+(\mathbf{r}) = \Delta_+$ and $\Delta_-(\mathbf{r}) = 0$ on the $p+ip$ side away from the domain wall, while $\Delta_+(\mathbf{r}) = 0$ and $\Delta_-(\mathbf{r}) = \Delta_-$ on the $p-ip$ side. The domain wall is then located where $|\Delta_+(\mathbf{r})| = |\Delta_-(\mathbf{r})|$. For the moment, assume both $\Delta_+(\mathbf{r})$ and $\Delta_-(\mathbf{r})$ are real and positive. The Bogoliubov-de Gennes (BdG) Hamiltonian of the superconductor then becomes gapless at momentum $\mathbf{k}_\pm = (0, \pm k_F)$ on the domain wall, as shown in Fig. 4(a). In the vicinity of the domain wall, the low energy BdG Hamiltonian at momentum $\mathbf{k}$ near $\mathbf{k}_+$ is

$$H_{BdG}(\mathbf{k}) = \begin{pmatrix} v_F(k_y - k_F) & v_\Delta k_x + im(\mathbf{r}) \\ v_\Delta k_x - im(\mathbf{r}) & -v_F(k_y - k_F) \end{pmatrix}, \tag{5}$$

where the basis is the Nambu basis $(c_{\mathbf{k}}, c^\dagger_{-\mathbf{k}})^{\mathrm{T}}$, $k_F = \sqrt{2m_0\mu}$ and $v_F = k_F/m_0$ are the electron Fermi momentum and Fermi velocity, $v_\Delta = [\Delta_+(\mathbf{r}) + \Delta_-(\mathbf{r})]/k_F$, and $m(\mathbf{r}) = \Delta_+(\mathbf{r}) - \Delta_-(\mathbf{r})$. The BdG Hamiltonian near $\mathbf{k}_- = -\mathbf{k}_+$ is simply the particle-hole transformation of Eq. (5) and describes exactly the same degrees of freedom.

The edge states on a single domain wall can be easily solved from the BdG Hamiltonian (5). For a domain wall perpendicular to the direction $\mathbf{n} = (\cos\varphi, \sin\varphi)$, the mass term

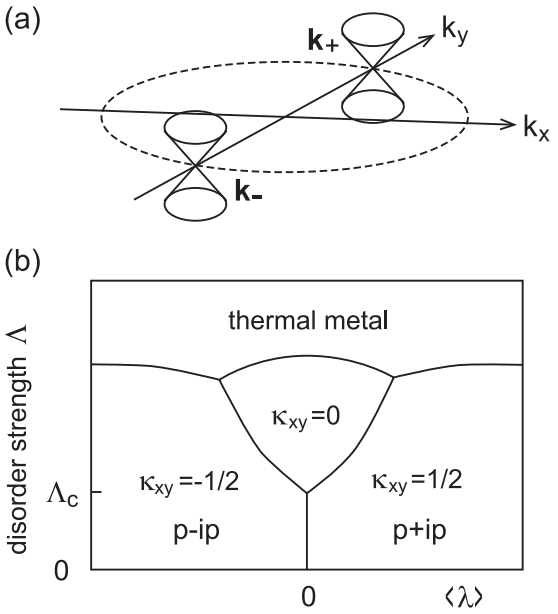

FIG. 4. (a) The low energy BdG bands on the domain wall between $p+ip$ and $p-ip$ superconductivity are two Dirac cones at $\mathbf{k}_+$ and $\mathbf{k}_-$, respectively. (b) Expected phase diagram for the disordered $p \pm ip$ superconducting system, where Λ is the disorder strength.

$m(\mathbf{r})$ can be approximated as a function of $x' = \mathbf{n}\cdot\mathbf{r}$ which is positive (negative) for $x' > 0$ ($x' < 0$), where we assume the domain wall is located at $x' = 0$. If we approximate v_Δ as a constant, the edge state at momentum k along the domain wall can be solved to be a chiral complex fermion

$$\psi_k = \begin{pmatrix} \cos\zeta \\ -\sin\zeta \end{pmatrix} e^{iky' + ip(k,\varphi)x' - \kappa(\varphi)\int_0^{x'} m(x'')dx''}, \tag{6}$$

where $y' = -x\sin\varphi + y\cos\varphi$ is the coordinate along the domain wall, $\kappa(\varphi) = (v_F^2\sin^2\varphi + v_\Delta^2\cos^2\varphi)^{-1/2}$, the angle $\zeta = \arctan[\frac{\kappa(\varphi)v_F\sin\varphi}{1+\kappa(\varphi)v_F\cos\varphi}]$, and $p(k,\varphi)$ is a real function of k and φ which is not important here. The energy of the edge mode is

$$\epsilon(k) = v(\varphi)(k - k_F\cos\varphi), \tag{7}$$

where $v(\varphi) = |v_F^{-1}\cos 2\zeta\cos\varphi + v_\Delta^{-1}\sin 2\zeta\sin\varphi|^{-1}$ is the edge state velocity, which oscillates between v_F and v_Δ as a function of φ with an oscillation period π. Therefore, the velocity $v(\varphi)$ depends on the direction of the domain wall. One can rewrite the complex fermion ψ_k as two chiral Majorana fermions $\chi_1 + i\chi_2$, then both χ_1 and χ_2 will propagate at the same velocity $v(\varphi)$. We note that if the pairing amplitudes $\Delta_+(\mathbf{r})$ and $\Delta_-(\mathbf{r})$ on the two sides of the domain wall have a phase difference $\varphi_\Delta \neq 0$, the edge state velocity will be shifted to $v(\varphi - \varphi_\Delta)$, and accordingly, $\mathbf{k}_\pm$ will be rotated to $\mathbf{k}_\pm = \pm(-k_F\sin\varphi_\Delta, k_F\cos\varphi_\Delta)$.

Regardless of the Nambu basis, the form of the Hamiltonian in Eq. (5) is no different from that of a charge conserved $2+1$D Dirac fermion with a spatial dependent mass $m(\mathbf{r})$. In fact, if the mass term varies slow enough so that $|\nabla m(\mathbf{r})/m(\mathbf{r})| < k_F$, we can define an emergent $U(1)$ symmetry for the BdG Hamiltonian at low energies as

$$c_{\mathbf{k}} \to e^{i\phi}c_{\mathbf{k}}, \quad c^\dagger_{-\mathbf{k}} \to e^{i\phi}c^\dagger_{-\mathbf{k}}, \tag{8}$$

where $\mathbf{k}$ and $-\mathbf{k}$ are momentums near $\mathbf{k}_+$ and $\mathbf{k}_-$, respectively. Such a $U(1)$ symmetry is analogous to the chiral $U(1)$ symmetry defined in Weyl semimetals [47,48], where electrons in different neighborhoods of the momentum space are associated with different phase rotations. As shown in Fig. 4(a), the two Dirac cones at $\mathbf{k}_\pm$ do not overlap with each other until the energy scale reaches the bulk gap $\Delta_\pm$ of the $p \pm ip$ superconductors. Therefore, as long as the energy scale under consideration is below a certain value Λ_c of the order of $\Delta_\pm$, the momentums $\mathbf{k}$ and $-\mathbf{k}$ in Eq. (8) are well separated, and the emergent $U(1)$ symmetry is well defined.

The configuration of random domains of $p \pm ip$ superconductivity is generically determined by a certain mass function $m(\mathbf{r})$, and the percolation of chiral Majorana fermions on the domain walls is entirely governed by the BdG Hamiltonian (5). We can define a disorder energy scale for the system as

$$\Lambda = \overline{v}/\ell_0, \tag{9}$$

where $\overline{v}$ is the mean value of the edge state velocity $v(\varphi - \varphi_\Delta)$, and ℓ_0 is the length scale of a single domain (i.e., the length of a link in the network model language [42]). When Λ is below Λ_c, our argument above shows the system has the emergent $U(1)$ symmetry defined in Eq. (8), so the system is in the A symmetry class [which is $U(1)$ symmetric] instead of the D symmetry class [43,44]. In other words, the two chiral Majorana fermions χ_1 and χ_2 on each domain wall behave as a single complex fermion with a conserved $U(1)$ charge. Accordingly, there will be only a single phase transition as a function of $\langle\lambda\rangle$ which changes κ_{xy} by 1, as shown in Fig. 4(b). Such a phase transition is similar to the Hall conductance plateau transition of integer quantum Hall (IQH) effect [42,49,50].

When $\Lambda > \Lambda_c$, the two Dirac cones at $\mathbf{k}_\pm$ begin to mix with each other, and the emergent $U(1)$ symmetry is lost. What remains is the $\mathbb{Z}_2^F$ symmetry of superconductors which takes $c_{\mathbf{k}} \to -c_{\mathbf{k}}$ and $c^\dagger_{-\mathbf{k}} \to -c^\dagger_{-\mathbf{k}}$ for all $\mathbf{k}$, and the system will be in the D symmetry class. In this case, the two chiral Majorana fermions will undergo two separate percolation transitions as a function of $\langle\lambda\rangle$, and an intermediate $\kappa_{xy} = 0$ phase arises. Furthermore, the D symmetry class allows the existence of a thermal metal phase for strong enough (π flux vortex) disorders, which has a divergent longitudinal thermal conductance κ_{xx} and a nonquantized κ_{xy}. The expected phase diagram is shown in Fig. 4(b).

We note that in this example, the absence of gapped trivial superconductor with $\kappa_{xy} = 0$ at zero disorder (due to single Fermi surface) is important for the emergent $U(1)$ symmetry to arise. Roughly speaking, this binds tightly the two chiral Majorana fermions between $p+ip$ and $p-ip$ regions within a single domain wall, so that they undergo percolation transitions together. This is different from the models where trivial superconductor is allowed in the absence of disorder, in which case the two chiral Majorana fermions between $p+ip$ and $p-ip$ regions will be spatially separated (by trivial regions) and percolate differently [51,52].

III. PAIRING PICTURE OF EMERGENT SYMMETRIES ON PFAFFIAN-ANTIPFAFFIAN DOMAIN WALL

The disordered $\nu = 5/2$ FQH system is similar to the example in Sec. II, in the sense that the ground state at zero disorder is believed to be restricted to either the Pf state or the APf state, which can be understood as $p + ip$ and $f - if$ superconductors of composite fermions, respectively. In this section, we shall illustrate the emergent symmetries of the domain wall between Pf and APf states in the composite fermion pairing picture. In the below, we shall show the emergent symmetries on the domain wall between Pf and APf under different energy scales based on the pairing picture.

A. Emergent $U(1) \times U(1)$ symmetry at energy scales $\Lambda_1 < \Lambda < \Lambda_2$

The Hamiltonian near the single Fermi surface of composite fermions in the first Landau level before pairing can be written as

$$H_0^{\rm cf} = \sum_{\mathbf{k}} v_F(|\mathbf{k}| - k_F) f_{\mathbf{k}}^\dagger f_{\mathbf{k}}, \tag{10}$$

where v_F and k_F are the Fermi velocity and Fermi momentum, respectively. At filling fraction $\nu = 5/2$, one has $k_F = 1/\ell_B$ by the Luttinger's theorem [53,54]. Depending on whether the filling fraction ν is either below or above ν_c, the Fermi surface will form either a $p + ip$ pairing (the Pf state) or a $f - if$ pairing (the APf state), as we have explained in Sec. I.

In the disordered $\nu = 5/2$ system consisting of Pf and APf domains, the pairing amplitude of composite fermions near a domain wall takes the form

$$\Delta(k) = \Delta_{\rm Pf}(\mathbf{r}) e^{i\theta_k} - \Delta_{\rm APf}(\mathbf{r}) e^{-3i\theta_k}, \tag{11}$$

where $\Delta_{\rm Pf}(\mathbf{r}) = \Delta_{\rm Pf}$, $\Delta_{\rm APf}(\mathbf{r}) = 0$ far away on the Pf side of the domain wall, and $\Delta_{\rm Pf}(\mathbf{r}) = 0$, $\Delta_{\rm APf}(\mathbf{r}) = \Delta_{\rm APf}$ far away on the APf side. The location of the domain wall is determined by $|\Delta_{\rm Pf}(\mathbf{r})| = |\Delta_{\rm APf}(\mathbf{r})|$. It is easy to show the BdG Hamiltonian of composite fermions is gapless at four momentums $\mathbf{k}_1 = -\mathbf{k}_2 = (-k_F \sin\varphi_\Delta, k_F \cos\varphi_\Delta)$ and $\mathbf{k}_3 = -\mathbf{k}_4 = (k_F \cos\varphi_\Delta, k_F \sin\varphi_\Delta)$ on the domain wall [Fig. 5(a)], where φ_Δ is the phase difference between $\Delta_{\rm Pf}(\mathbf{r})$ and $\Delta_{\rm APf}(\mathbf{r})$. By defining $v_\Delta = (|\Delta_{\rm Pf}(\mathbf{r})| + |\Delta_{\rm APf}(\mathbf{r})|)/k_F$ and the mass term $m(\mathbf{r}) = |\Delta_{\rm Pf}(\mathbf{r})| - |\Delta_{\rm APf}(\mathbf{r})|$, the low energy BdG Hamiltonian in the vicinity of $\mathbf{k}_i$ $(1 \leqslant i \leqslant 4)$ takes the form of Dirac fermions similar to Eq. (5). Following the argument in Sec. II, when the energy scale is below a certain value Λ_2 around the order of $\Delta_{\rm APf}$ or $\Delta_{\rm Pf}$, the four Dirac cones of the BdG band are well separated in momentum space, and one can define two emergent $U(1)$ symmetries

$$f_{\mathbf{k}} \to e^{i\phi} f_{\mathbf{k}}, \quad f_{-\mathbf{k}}^\dagger \to e^{i\phi} f_{-\mathbf{k}}^\dagger \tag{12}$$

for $\mathbf{k}$ near $\mathbf{k}_1 = -\mathbf{k}_2$ and $\mathbf{k}$ near $\mathbf{k}_3 = -\mathbf{k}_4$, respectively. The two emergent $U(1)$ symmetries are independent of each other, so the total emergent symmetry is $U(1) \times U(1)$.[2] For a domain wall perpendicular to $\mathbf{n} = (\cos\alpha, \sin\alpha)$, the Dirac cone at $\mathbf{k}_1 = -\mathbf{k}_2$ yields a complex chiral fermion ψ_k^a with velocity $v_a = v(\varphi - \varphi_\Delta)$, while the Dirac cone at $\mathbf{k}_3 = -\mathbf{k}_4$ yields a complex chiral fermion ψ_k^a with velocity $v_b = v(\varphi - \varphi_\Delta + \pi/2)$, where $v(\varphi)$ is defined below Eq. (7). By rewriting the two complex chiral fermions into four chiral Majorana fermions as $\psi^a = \chi_1 + i\chi_2$ and $\psi^b = \chi_3 + i\chi_4$, we can write down an action of the domain wall:

$$S = \int dt dx \sum_{I=1}^{4} \chi_I (i\partial_t - i v_I \partial_x) \chi_I, \tag{13}$$

where $v_I = (v_a, v_a, v_b, v_b)$, x is the spatial coordinate along the domain wall, and the origin of momentum k is properly redefined. The emergent $U(1) \times U(1)$ symmetry then corresponds to the SO(2) rotation between χ_1 and χ_2 and the SO(2) rotation between χ_3 and χ_4. Since the only energy scale within the first Landau level is the Coulomb interaction $e^2/\epsilon\ell_B$ where ϵ is the dielectric constant, we expect both v_F and v_Δ, and thus v_a and v_b, to be of order $e^2/\epsilon\ell_B\hbar k_F \sim e^2/\epsilon\hbar$. The reason we expect the energy scale for the emergent $U(1) \times U(1)$ symmetry to break down is

$$\Lambda_2 \lesssim e^2/\epsilon\ell_B. \tag{14}$$

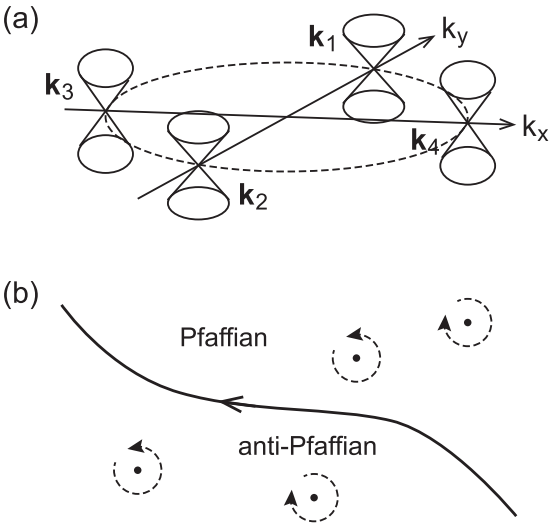

FIG. 5. (a) The low energy BdG bands on the domain wall between Pf and APf states consist of four Dirac cones at $\mathbf{k}_i$ $(1 \leqslant i \leqslant 4)$. (b) Top view of a domain wall. The pairing phase difference φ_Δ on the domain wall acquires fluctuations from random $\pm\pi$ flux vortices on the Pf or APf side and other small fluctuations.

B. Emergent SO(4) symmetry at energy scales $\Lambda < \Lambda_1$

The above $U(1) \times U(1)$ emergent symmetry is further enhanced in the presence of spatial or temporal fluctuations of the pairing phase difference $\varphi_\Delta = \arg(\Delta_{\rm Pf}/\Delta_{\rm APf})$, which controls the velocities v_a and v_b of chiral Majorana fermions. Such fluctuations are generically present due to interactions,

[2]The $U(1) \times U(1)$ symmetry is effectively the same as SO(2) × SO(2). The SO(2) symmetry is the rotational symmetry that bonds two chiral Majorana-Weyl fermions together. We also denote $U(1)$ symmetry to make connection to the A class of Cartan notations in electronic disordered systems.

disorders, and finite temperatures. To see the enlarging of the emergent symmetry, we can rewrite the action as

$$S = \int dtdx \sum_{I=1}^{4} [\chi_I(i\partial_t - i\bar{v}\partial_x)\chi_I - i\delta v_I(x,t)\chi_I\partial_x\chi_I], \tag{15}$$

where $\bar{v} = \frac{1}{2\pi}\int_0^{2\pi} v(\varphi)d\varphi$ is the mean edge state velocity, while $\delta v_I(x,t) \approx \frac{v_F - v_\Delta}{2}\cos[\varphi_\Delta(x,t) - \varphi_{0I}]$ is the anisotropic velocity of χ_I, where φ_{0I} is some constant. The correlation function of δv_I is thus closely related to the correlation function of φ_Δ, namely, $\langle\delta v_I(x)\delta v_I(x')\rangle \propto \langle\cos[\varphi_\Delta(x) - \varphi_\Delta(x')]\rangle$, while the mean value $\langle\delta v_I(x)\rangle = 0$.

At zero disorder, the Berezinskii-Kosterlitz-Thouless (BKT) mechanism [55,56] will yield either a power law or an exponential correlation $\langle e^{i\varphi_\Delta(x) - i\varphi_\Delta(x')}\rangle$ for temperature T below or above the BKT transition temperature $T_{\rm BKT}$, therefore

$$\langle\delta v_I(x)\delta v_I(x')\rangle = \begin{cases} W_v|x-x'|^{-2\eta} & (T < T_{\rm BKT}), \\ W_v\xi_v^{-1}e^{-|x-x'|/\xi_v} & (T > T_{\rm BKT}), \end{cases}$$

where W_v characterises the strength of the correlation, $\eta > 0$, and ξ_v depends on interactions. In the presence of disorders, random $\pm\pi$ flux vortices generically arise in both Pf and APf domains and are pinned by disorders. Due to these vortices, $\varphi_\Delta(\mathbf{r})$ at $\mathbf{r}$ on the domain wall becomes $\varphi_\Delta(\mathbf{r}) = \varphi_\Delta^0 + \sum_j \eta_j\theta(\mathbf{r} - \mathbf{r}_j)/2$, where φ_Δ^0 are small fluctuations, $\mathbf{r}_j$ is the 2D spatial coordinate of the jth vortex, $\theta(\mathbf{r})$ stands for the polar angle of $\mathbf{r}$ in polar coordinates, and $\eta_j = \pm 1$ for $\pm\pi$ ($\mp\pi$) vortices on the Pf (APf) side of the domain wall. Given $\mathbf{r}_j$ and η_j fully random, one would have

$$\langle\delta v_I(x)\delta v_I(x')\rangle = W_v\delta(x - x'),$$

where x, x' denote the 1D coordinate along the domain wall. In any case, one would find the scaling dimension of W_v to be negative, which is either $d_v = -2\eta$ or $d_v = -1$. The renormalization group (RG) equation for W_v is given by

$$\frac{dW_v}{d\log\Lambda} = -d_v W_v, \tag{16}$$

where Λ is the energy scale of the physical process under consideration. Therefore, W_v is irrelevant at low energies, and the second term in Eq. (15) can be dropped at low energies. The remaining action then has an enlarged emergent symmetry SO(4), i.e., rotations in the four-dimensional space spanned by χ_I ($1 \leqslant I \leqslant 4$). This conclusion can also be drawn by examining correlations of $\delta v_I(x,t)$ in the time direction. The energy scale for the emergent SO(4) symmetry to break down is roughly

$$\Lambda_1 \sim \bar{v}(\bar{v}^2/W_v^*)^{-1/d_v}, \tag{17}$$

where W_v^* is the value of W_v at the ultraviolet (UV) cutoff. In general, we expect $\Lambda_1 < \Lambda_2$, since the fluctuations of φ_Δ usually appear at longer distances compared to ℓ_B.

When the $\nu = 5/2$ FQH system forms a random domain of Pf and APf states, an energy scale of disorder strength can be defined as $\Lambda = \bar{v}/\ell_0$ similar to Eq. (9), where ℓ_0 is the size of a single Pf or APf domain, or the length of a link when formulated in network models [42]. In particular, the inter-domain-wall tunneling area indicated by the dashed circle in Fig. 1 roughly has a length scale around ℓ_0, therefore all the scattering angles α_I ($1 \leqslant I \leqslant 4$) are determined at the energy scale $\Lambda = \bar{v}/\ell_0$. The expected phase diagram of the system is then as shown in Fig. 2. When $\Lambda < \Lambda_1$, the emergent SO(4) symmetry enforces all the four chiral Majorana fermions χ_I ($1 \leqslant I \leqslant 4$) to have the same scattering angles α_I, so there is only a single phase transition from Pf state to APf state with respect to ν. When $\Lambda_1 < \Lambda < \Lambda_2$, the emergent symmetry is lowered to $U(1) \times U(1)$, which only ensures χ_1 is identical to χ_2, and χ_3 is identical to χ_4. Therefore, there are two phase transitions with respect to ν, and an intermediate $\kappa_{xy} = 5/2$ phase arises. For strong disorder strengths $\Lambda > \Lambda_2$, only the $\mathbf{Z}_2$ symmetry $f_\mathbf{k} \to -f_\mathbf{k}$ remains, and the system is in the D symmetry class. The system may undergo four phase transitions with κ_{xy} changing by $1/2$ each time, or it may enter the thermal metal phase. However, if the energy scale Λ_2 is comparable to the bulk gap of Pf and APf states, the analysis for $\Lambda > \Lambda_2$ may become invalid, since the concept of domains of Pf and APf states is no longer well defined. As a result, the phases of $\kappa_{xy} = 2$ and 3 may not exist.

We note the phase diagram we predicted in Fig. 2 differs from that predicted in Refs. [23,24] in some aspects. This is due to the low energy emergent symmetries we identified in the above, which are not fully considered in the two earlier papers. In particular, we expect the thermal metal phase to arise only beyond disorder energy scale Λ_2, since the system is effectively not in D class for $\Lambda < \Lambda_2$ where there is a $U(1) \times U(1)$ or $SO(4)$ emergent symmetry. Besides, in Refs. [23,24] the authors suggest the identification of the $\kappa_{xy} = 2, 5/2$, and 3 phases with known FQH candidates, the $K = 8$, PH-Pf, and 113 states [57]. Here we shall not attempt to make such identifications in this work, as the three phases in the phase diagram Fig. 2 do not exist at zero disorder, therefore may have bulk theories different from the above known FQH states at zero disorders. Instead, we leave this problem of phase identification for future studies.

Although we do not attempt to identify all phases in phase diagrams, we can still identify the spin TQFTs for these Pf/PH-Pf/APf states (in Appendix A), which provides essential data to confirm the phases and their underlying topological orders in the future.

IV. EDGE THEORY OF DISORDERED PFAFFIAN-ANTIPFAFFIAN DOMAIN WALL

In this section, we give an understanding of emergent symmetries on the domain wall between Pf and APf states from the usual FQH edge theory formalism, where the physical meaning of disorders becomes clearer. We shall also show how the charged modes are gapped out, leaving a domain wall with four charge neutral chiral Majorana fermions. Previous analysis of a domain wall between Pf and APf states limited to Abelian sector can be found in Refs. [58,59], while here we carry out the analysis under the most possible physical assumptions consistent with the experiments, also suitable for non-Abelian topological orders (see Appendices B–E). Furthermore, we reveal the existence of a nonlocal topological degeneracy associated with multiple domain walls in Sec. V.

The $1+1$D edge theory of the domain wall between Pf and APf states can be derived from their bulk theories

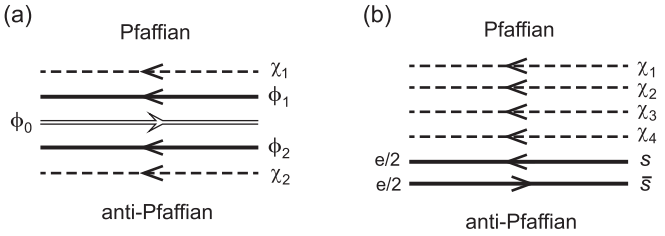

FIG. 6. (a) Edge modes on the domain wall between Pf state and APf state before charge sector is gapped out, which include two left-moving chiral Majorana modes χ_1 and χ_2, two left-moving charge $e/2$ level-2 chiral bosons, and a right-moving charge e level-1 chiral boson. (b) After a disorder induced recombination, the modes between Pf and APf states become four neutral chiral Majorana modes χ_I ($1 \leqslant I \leqslant 4$), and two opposite chiral boson modes of charge $e/2$ (semions) which gap themselves out due to interactions.

(Appendices A and B) [33], which has an effective action

$$S = S_\phi + S_\chi + S_{\rm int} + S_d,$$
$$S_\phi = \int \frac{dtdx}{4\pi} \sum_{I,J=0}^{2} (K_{IJ}\partial_t\phi_I\partial_x\phi_J - V_{IJ}\partial_x\phi_I\partial_x\phi_J), \quad (18)$$
$$S_\chi = \int dtdx \sum_{I=1}^{2} \chi_I(i\partial_t - iv_I\partial_x)\chi_I,$$

where the K matrix and the chiral boson basis are given by

$$K = \begin{pmatrix} 2 & 0 & 0 \\ 0 & -1 & 0 \\ 0 & 0 & 2 \end{pmatrix}, \quad \begin{pmatrix} \phi_1 \\ \phi_0 \\ \phi_2 \end{pmatrix}. \quad (19)$$

V_{IJ} is the velocity matrix which is positive definite and symmetric, and $S_{\rm int}$ and S_d denote the contributions of other interactions and disorders, respectively. As shown in Fig. 6(a), ϕ_1 and ϕ_2 are two left-moving charge $e/2$ level 2 chiral bosons, ϕ_0 is a right-moving charge e level 1 chiral boson which is identical to a complex fermion (electron), while χ_1 and χ_2 are two left-moving neutral chiral Majorana fermions with velocities $v_1 > 0$ and $v_2 > 0$, respectively. The edge modes ϕ_1 and χ_1 come from the Pf state, while ϕ_0, ϕ_2, and χ_2 are from the APf state [14,15,33]. Note that Fig. 6(a) is only illustrative and does not represent the physical positions of the five modes on the domain wall. The total electron charge density of the domain wall is given by $\rho = (e/2\pi)q_I\partial_x\phi_I$ (hereafter we assume repeated indices I are automatically summed), where $q_I = (1,1,1)^{\rm T}$ is the charge vector. Accordingly, the vertex operator $e^{i\phi_I}$ ($e^{-i\phi_I}$) creates (annihilates) a fractionalized quasiparticle of charge $t_I = (K^{-1})_{IJ}q_J$ in units of e. Therefore, V_{IJ} can be viewed as interactions between charge densities $\partial_x\phi_I/2\pi$ and $\partial_x\phi_J/2\pi$.

A. Emergent $U(1) \times U(1)$ symmetry at energy scales $\Lambda_1 < \Lambda < \Lambda_2$

For convenience of analysis, we first make an $SL(3,\mathbb{Z})$ transformation $K' = U^{-1T}KU^{-1}$ to the K matrix to a new basis $\phi_s = \phi_1$, $\phi_{\bar{s}} = \phi_2 + \phi_0$ and $\phi_n = 2\phi_2 + \phi_0$, after which the K matrix becomes (Appendix D)

$$K' = \begin{pmatrix} 2 & 0 & 0 \\ 0 & -2 & 0 \\ 0 & 0 & 1 \end{pmatrix}, \quad \begin{pmatrix} \phi_s \\ \phi_{\bar{s}} \\ \phi_n \end{pmatrix}. \quad (20)$$

Accordingly, the charge vector is transformed to $q'_I = (U^{-1}q)_I = (1,1,0)^{\rm T}$, and the velocity matrix becomes $V'_{IJ} = (U^{-1T}VU^{-1})_{IJ}$. In this basis, the chiral bosons ϕ_s of level 2 and $\phi_{\bar{s}}$ of level -2 have a correspondence with charge $e/2$ semions in the Pf bulk and charge $-e/2$ antisemions in the APf bulk, respectively, while ϕ_n is a charge neutral level 1 chiral boson identical to a complex fermion [14,15]. The charged sector of the domain wall is therefore a nonchiral double-semion theory, while the neutral sector is fully chiral.

The nonchiral charged sector of the domain wall can be properly gapped out by interactions [30,31,46]. Generically, the allowed interaction terms on the domain wall must be bosonic (statistically trivial), nonfractionalized, nonchiral, and charge conserving (Appendix C), which constrains the most relevant interaction term to be (Appendix D)

$$S_{\rm int} = \int dtdx[g\, e^{2i(\phi_s+\phi_{\bar{s}})} + {\rm H.c.}], \quad (21)$$

where g is the coupling constant. Without loss of generality, hereafter we shall assume $g > 0$ is real. The scaling dimension of the vertex operator $e^{2i(\phi_s+\phi_{\bar{s}})} = e^{2i(\phi_1+\phi_2+\phi_0)}$, and thus the scaling dimension of g, depend on the velocity matrix V_{IJ}. For instance, if the original velocity matrix V_{IJ} is symmetric under exchange of ϕ_1 and ϕ_2, namely $V_{11} = V_{22}$ and $V_{01} = V_{02}$, the dimension of g can be obtained as $d_g = 2 - 2\sqrt{\frac{2V_{00}+V_{11}+V_{12}-4V_{01}}{2V_{00}+V_{11}+V_{12}+4V_{01}}}$. In particular, when $V_{01} = V_{02} > 0$, we have $d_g > 0$, and the interaction (21) is relevant and will gap out ϕ_s and $\phi_{\bar{s}}$. This is likely to be the case, since V_{IJ} mainly comes from Coulomb repulsions between charges $\partial_x\phi_I$ and $\partial_x\phi_J$. However, we note that even if interaction (21) is perturbatively irrelevant, it can still gap out ϕ_s and $\phi_{\bar{s}}$ in the strongly interacting nonperturbative regime [30]. In either case, ϕ_s and $\phi_{\bar{s}}$ are gapped out by condensation of semion antisemion pairs $s\bar{s}$ on the domain wall, which yields a nonzero expectation value

$$\langle e^{2i(\phi_s+\phi_{\bar{s}})}\rangle = 1, \quad (22)$$

and minimizes the interaction energy in Eq. (21). As we shall show in Sec. V, such a condensation also induces additional zero modes associated with the domain walls.

Given ϕ_s and $\phi_{\bar{s}}$ gapped out, the remaining edge theory only contains a level 1 left-moving neutral chiral boson ϕ_n with a renormalized velocity V'_{nn}, and two left-moving chiral Majorana fermions χ_1 and χ_2 with velocities v_1 and v_2. As we argued in Sec. III, the domain wall should already exhibit a $U(1) \times U(1)$ emergent symmetry before we further add any disorder terms S_d. We expect this to result from a combined approximate discrete $\mathbb{Z}_2$-symmetry $R_2\mathcal{C}$, which is respected by the neighborhood of the domain wall, where R_2 is the π rotation (twofold rotation) about a point on the domain wall, and $\mathcal{C}$ is the particle-hole transformation in the first Landau

level [34]. Such a symmetry transformation exchanges ϕ_1 with ϕ_2 and χ_1 with χ_2, therefore ensures $v_1 = v_2$. The domain wall then has two independent $U(1)$ symmetries, which are the $U(1)$ phase rotation of $e^{i\phi_n}$ and the SO(2) flavor rotation symmetry of Majorana modes $(\chi_1, \chi_2)^{\mathrm{T}}$, respectively.

One may concern that our definition of the neutral mode $\phi_n = 2\phi_2 + \phi_0$ is asymmetric under exchange of ϕ_1 and ϕ_2, and does not respect the $R_2\mathcal{C}$ symmetry. In fact, due to the condensation in Eq. (22), we have $2(\phi_s + \phi_{\bar{s}}) = 2(\phi_1 + \phi_2 + \phi_0) = 0 \,(\mathrm{mod}\, 2\pi)$, or $2\phi_2 + \phi_0 = -2\phi_1 - \phi_0 \,(\mathrm{mod}\, 2\pi)$. Therefore, ϕ_n becomes $-\phi_n$ up to multiples of 2π under $R_2\mathcal{C}$, and the $R_2\mathcal{C}$ symmetry is still respected.

A small violation of $R_2\mathcal{C}$ symmetry due to small distortions of the domain wall will not affect the $U(1) \times U(1)$ emergent symmetry. This is because such perturbations only generate a random velocity difference $\delta v(x) = v_1(x) - v_2(x)$ between v_1 and v_2, which satisfies $\langle \delta v(x) \delta v(x') \rangle \propto \delta(x - x')$. By an RG analysis similar to that done in Sec. III B, one would find $\delta v(x)$ is an irrelevant perturbation.

The $U(1) \times U(1)$ emergent symmetry will, however, be lost when the domain wall is severely bent or distorted, namely, when the size of a single domain ℓ_0 is comparable to ℓ_B. This leads to a breakdown energy scale of the emergent $U(1) \times U(1)$ symmetry roughly around $\Lambda_2 \lesssim e^2/\epsilon \ell_B$, which is in agreement with our estimation in Sec. III.

B. Emergent SO(4) symmetry at energy scales $\Lambda < \Lambda_1$

In the presence of disorders, a disorder term S_d arises from random backscattering of electrons on the domain wall. Such disorder may come directly from chemical potential fluctuations on the domain wall, or indirectly from charge $\pm e/4$ quasiparticles in Pf and APf domains forced to arise by the local filling fraction $\nu(\mathbf{r})$. There are three electron creation operators one could write down on the domain wall between Pf and APf: $\chi_1 e^{2i\phi_1}$, $\chi_2 e^{2i\phi_2}$, and $e^{-i\phi_0}$ [14,15], each of which has charge e and fermionic statistics. The most relevant backscattering action can then be expressed as

$$S_d = \int dt dx [\xi_1(x)\chi_1 e^{2i\phi_1 + i\phi_0} + \xi_2(x)\chi_2 e^{2i\phi_2 + i\phi_0} + \mathrm{H.c.}], \tag{23}$$

where $\xi_I(x)$ are random functions satisfying $\overline{\xi_I^*(x)\xi_J(x)} = W_I \delta_{IJ} \delta(x - x')$ $(I = 1,2)$ and have zero means. Since ϕ_s and $\phi_{\bar{s}}$ are gapped out, one can then rewrite the vertex operators in the new basis as $e^{2i\phi_1 + i\phi_0} = e^{2i(\phi_s + \phi_{\bar{s}})} e^{-i\phi_n}$ and $e^{2i\phi_2 + i\phi_0} = e^{i\phi_n}$, and then replace $e^{2i(\phi_s + \phi_{\bar{s}})}$ by its expectation value 1. The disorder term then becomes

$$S_d = \int dt dx [\xi_1(x)\chi_1 e^{-i\phi_n} + \xi_2(x)\chi_2 e^{i\phi_n} + \mathrm{H.c.}]. \tag{24}$$

The scaling dimension of the disorder strengths W_1 and W_2 can be easily found to be $d_1 = d_2 = 1/2$, therefore the disorder term S_d is a relevant perturbation. The problem can be solved by redefining the chiral boson mode ϕ_n as two chiral Majorana fermions $e^{i\phi_n} = \chi_3 + i\chi_4$. The disorder term S_d can then be rewritten as

$$S_d = \int dt dx \, \omega_a(x) \chi^{\mathrm{T}} T^a \chi,$$

where $\chi = (\chi_1, \chi_2, \chi_3, \chi_4)^{\mathrm{T}}$ are the Majorana fields, T^a $(1 \leqslant a \leqslant 6)$ are the SO(4) group generators, and we have defined $\omega_a(x) = (0, \mathrm{Re}\xi_1(x), \mathrm{Im}\xi_1(x), \mathrm{Re}\xi_2(x), \mathrm{Im}\xi_2(x), 0)$. By doing a unitary transformation $\chi(x) = O(x)\chi'(x)$ where $O(x) = P \exp(-\frac{i}{\bar{v}} \int_{-\infty}^{x} dx' \omega_a(x') T^a)$, one can eliminate S_d in the action [14,15,45], with the rest action taking the form

$$S = \int dt dx [\chi'^{\mathrm{T}}(i\partial_t - i\bar{v}\partial_x)\chi' - i\chi'^{\mathrm{T}} \delta v'(x) \partial_x \chi'], \tag{25}$$

where $\bar{v} = (v_1 + v_2 + 2V'_{nn})/4$ is the mean velocity, while $\delta v'(x) = O(x)^{\mathrm{T}}(v - \bar{v})O(x)$ is the randomly rotated velocity anisotropy, with the original velocity matrix $v = \mathrm{diag}(v_1, v_2, V'_{nn}, V'_{nn})$. The correlation of $\delta v'(x)$ is short ranged, which can be estimated to be $\mathrm{tr}\overline{\delta v'(x)\delta v'(x')} \sim e^{-(W_1^* + W_2^*)|x - x'|/\bar{v}^2} \sim W_v \delta(x - x')$, where W_I^* is the UV value of the disorder strengths W_I $(I = 1,2)$. It is then straightforward to see the scaling dimension of W_v is $d_v = -1 < 0$, so the $\delta v'(x)$ term is irrelevant. As a result, the action S gains an SO(4) emergent symmetry of rotation of four chiral Majorana fermions χ'_I at low energies. The breakdown energy scale of the SO(4) emergent symmetry can be estimated as $\Lambda_1 \sim (W_1^* + W_2^*)/\bar{v}$. We thus reach the same conclusion as that in Sec. III.

V. NONLOCAL TOPOLOGICAL DEGENERACY AND HEAT CAPACITY

We have been focusing on the neutral chiral Majorana fermion sector of the domain walls between Pf and APf so far. In this section, we shall show the charged nonchiral double-semion sector (ϕ_s and $\phi_{\bar{s}}$), although gapped out, still contributes a ground state degeneracy (GSD), which scales up exponentially with respect to the number of $1 + 1$D compact domain walls.[3] Thus, these ground states participate in the low energy physics such as the specific heat.

The GSD due to gapped ϕ_s and $\phi_{\bar{s}}$ on compact domain walls between Pf and APf can be most easily seen from the condensation condition of Eq. (22), which is required by the minimization of interaction energy (21). On each compact domain wall, Eq. (22) is satisfied by two saddle point solutions[4]

$$\phi_s + \phi_{\bar{s}} = 0 \text{ or } \pi \,(\mathrm{mod}\, 2\pi). \tag{26}$$

One can understand $\phi_s + \phi_{\bar{s}}$ as the phase angle of the semion antisemion pairing order parameter. When there is just one compact domain wall, $\phi_s + \phi_{\bar{s}} = 0$ and π describe the same physical ground state, since they only differ by a global redefinition of $\phi_s \to \phi_s + \pi$. When there are two compact domain walls far apart from each other, the angle $\phi_s + \phi_{\bar{s}}$ on

[3] By a $1 + 1$D compact domain wall (or interface), we mean that a 1D spatial closed domain wall, homotopic equivalent to a spatial S^1 circle, without $0 + 1$D ends.

[4] More precisely, here we mean the zero modes $\phi_{0,s}$ and $\phi_{0,\bar{s}}$ can be pinned down thus localized at strong coupling due to nonperturbative effects. Their conjugate momenta, winding modes $P_{\phi,s}$ and $P_{\phi,\bar{s}}$, actually fluctuate and can hop in the quantized winding mode Hilbert space. See Appendix D on the derivation of zero modes/winding modes counting and GSD calculations.

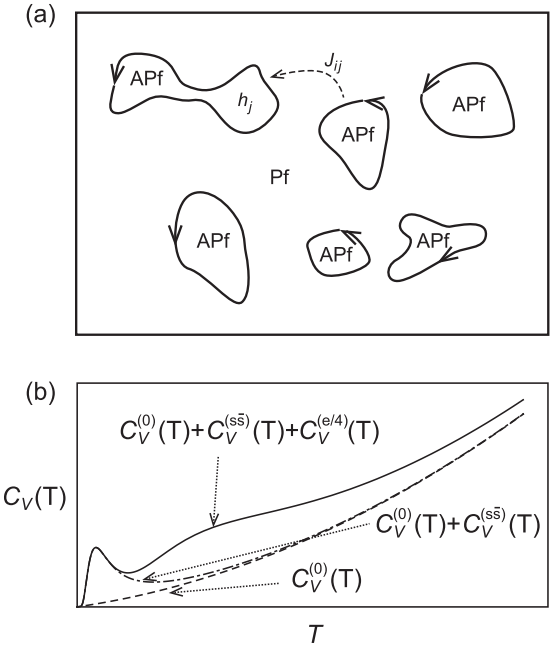

FIG. 7. (a) The double-semion sector of N_D domain walls between Pf and APf states contribute a GSD 2^{N_D-1}. The GSD are lifted into low energy modes by the double semion hoppings J_{ij} and local energy splittings h_i, which are nonzero when the sizes and distances of the domain walls are finite. (b) Heat capacity of the system, which exhibit two peaks (solid line) due to contributions of the double-semion GSD ($C_V^{(s\bar{s})}(T)$) and charge $e/4$ non-Abelian quasiparticles ($C_V^{(e/4)}(T)$).

each domain wall can be either 0 or π. Again, a global π shift of $\phi_s+\phi_{\bar{s}}$ on both domain walls does not change the physical state. The phase difference of $\phi_s+\phi_{\bar{s}}$ between the two domain walls, however, is physically meaningful, which can be either 0 or π. This is analogous to the phase difference of two superconductors in a Josephson junction. Therefore, the system with two domain walls has GSD = 2 degenerate ground states in the double-semion sector corresponding to $\phi_s+\phi_{\bar{s}}$ phase differences 0 and π, respectively.

In general, when there are N_D compact domain walls far away from each other [Fig. 7(a)], each domain wall could have $\phi_s+\phi_{\bar{s}}=0$ or π, and a global π shift on all domain walls does not alter the ground state. Therefore, there are GSD $=2^{N_D-1}$ degenerate ground states in the double-semion sector. A more detailed derivation of the GSD can be found in Appendix D and Ref. [30].

By viewing $\tau_z^j=e^{i(\phi_s+\phi_{\bar{s}})|_j}=\pm1$ on the jth domain wall as an Ising spin, the double-semion sector GSD can be approximately modeled as the degrees of freedom of n Ising spins up to a global flip of all spins [60]. When quantum fluctuations of $\phi_s+\phi_{\bar{s}}$ are considered, the Ising spins acquire a local energy splitting $h_j\propto e^{-L_j/\xi_s}$ and a spin interaction between domain walls $J_{ij}\propto e^{-L_{ij}/\xi_s}$, where L_j is the size of the jth domain wall, and L_{ij} is the distance between the ith and jth domain walls. Physically, h_j is the tunneling between potential wells at $\phi_s+\phi_{\bar{s}}=0$ and π, while J_{ij} is the hopping of semion antisemion pairs $s\bar{s}$ between domain walls i and j. The N_D Ising spins then form a $2+1$D transverse field Ising model with an effective Hamiltonian

$$H_{s\bar{s}}=\sum_{j=1}^{N_D}h_j\tau_x^j+\sum_{1=i<j}^{N_D}J_{ij}\tau_z^i\tau_z^j, \tag{27}$$

subject to a restriction $\prod_{j=1}^{N_D}\tau_x^j=1$ which eliminates the global spin flip redundancy. These charge neutral low energy modes together with chiral Majorana fermions on the domain walls constitute the effective theory of the system under disorders.

One effect of $H_{s\bar{s}}$ is its contribution to heat capacity at low temperatures, as noted by Ref. [60]. For instance, in the limit $J_{ij}\to0$, the heat capacity at temperature $T=1/k_B\beta$ due to $H_{s\bar{s}}$ is

$$C_v^{(s\bar{s})}=k_B\beta^2\frac{\partial^2\ln(\mathrm{tr}e^{-\beta H_{s\bar{s}}})}{\partial\beta^2}=\sum_{j=1}^{N_D}\frac{h_j^2}{k_BT^2}\,\mathrm{sech}^2\left(\frac{h_j}{k_BT}\right). \tag{28}$$

The total heat capacity is then given by $C_v(T)=C_v^{(0)}(T)+C_v^{(s\bar{s})}(T)$, where $C_v^{(0)}(T)\approx\gamma_1T+\gamma_2T^2$ is the contribution from chiral Majorana fermions and phonons. In particular, the GSD Hamiltonian $H_{s\bar{s}}$ contributes a peak at k_BT around the order of magnitude of h_j and J_{ij}, as shown in Fig. 7(b), and the peak height is proportional to the number of domain walls N_D. Since both h_j and J_{ij} are exponentially small, the temperature of the peak is expected to be low. Furthermore, when the system is n electrons away from filling fraction $\nu=5/2$, there will be $N_{e/4}\approx4n$ non-Abelian quasiparticles of charge $e/4$, which contribute another factor $2^{(N_{e/4}/2)-1}$ to the GSD. When the hopping and mobility among these quasiparticles are taken into account, they will also contribute a heat capacity $C_v^{(e/4)}(T)$ peaked at k_BT around the energy scale of their hopping. Since the $e/4$ quasiparticles are pointlike and free to move, we expect their hopping to be much larger than that between two domain walls. As a result, the total heat capacity $C_v(T)=C_v^{(0)}(T)+C_v^{(s\bar{s})}(T)+C_v^{(e/4)}(T)$ will exhibit a lower peak due to double-semion GSD and a higher peak due to charge $e/4$ non-Abelian quasiparticles, as illustrated by the solid line in Fig. 7(b). This provides a way to tell whether the $\nu=5/2$ FQH system in the experiment is formed by a large number of random Pf and APf domains.

In addition, these almost zero energy modes will also contribute to the longitudinal thermal conductance κ_{xx}. They will however not affect κ_{xy}, since they have a nonchiral nature and are decoupled from chiral Majorana fermions on the domain walls. Therefore, all our earlier conclusions about κ_{xy} remain unchanged.

Lastly, we remark that when there are closed Pf|APf|Pf domain walls, namely, narrow Corbino rings of APf in the background of Pf, such domain walls may contain the gapped non-Abelian sector that contributes to the GSD differently (see Appendix E and Ref. [61]). In practice, such domain walls may rarely occur. If they are present for some reason, the above physical picture still holds, except that the scaling behavior of the GSD with respect to the number of domain walls may be different.

VI. CONCLUSION AND DISCUSSION

In conclusion, under the assumption that the disordered $\nu = 5/2$ FQH system is formed by random domains of Pf and APf states, we studied the low energy theory and emergent symmetries of the domain walls separating Pf and APf and proposed a possible phase diagram for the system with respect to disorders. The study is aimed at explaining the thermal Hall conductance $\kappa_{xy} = 5/2$ in the $\nu = 5/2$ FQH state as revealed by the recent experiment [19], while a clean Pf (APf) state has $\kappa_{xy} = 7/2$ ($\kappa_{xy} = 3/2$). When random domains of Pf and APf are formed in the system, each domain wall contains four chiral Majorana fermion modes, and it has been suggested that the percolation of these chiral Majorana fermions on the domain walls in the bulk may stabilize a $\kappa_{xy} = 5/2$ phase under disorders [23,24]. In this work, we studied in details the domain wall edge theory between Pf and APf. In particular, we show the theory has an SO(4) emergent symmetry at low energy scales $\Lambda < \Lambda_1$, which is lowered to $U(1) \times U(1)$ emergent symmetry at intermediate energy scales $\Lambda_1 < \Lambda < \Lambda_2$, and is then lowered to the $\mathbb{Z}_2^F$ fermion parity symmetry at high energies $\Lambda > \Lambda_2$. The energy scale dependent emergent symmetries enable us to propose a more specific phase diagram Fig. 2 regarding the mean filling fraction ν and the disorder energy scale $\Lambda = \bar{v}/\ell_0$, where $\bar{v}$ is the mean velocity of chiral Majorana fermions on the domain walls, and ℓ_0 is the rough size of a single Pf or APf domain. When $\Lambda < \Lambda_1$, the system involves only a single phase transition from Pf state to APf state with respect to ν, as forced by the emergent SO(4) symmetry. When $\Lambda_1 < \Lambda < \Lambda_2$, the $U(1) \times U(1)$ emergent symmetry allows two phase transitions with respect to ν, and an intermediate $\kappa_{xy} = 5/2$ phase arises between Pf and APf phases. Under strong disorders $\Lambda > \Lambda_2$, the system may undergo four phase transitions with ν, each of which changes κ_{xy} by $1/2$, or the system may become a gapless thermal metal with nonquantized κ_{xy}.

We also show the gapped double semion sector of the domain wall between Pf and APf contributes a GSD 2^{N_D-1} when there are N_D compact domain walls. When the N_D domain walls are small and spatially close, these GSD may be lifted to neutral low energy modes, which contributes a peak to the heat capacity C_v and increases the longitudinal thermal conductance κ_{xx}. This may be used to detect whether the system consists of a large number of domain walls in experiments.

However, we emphasize that the explanation for $\kappa_{xy} = 5/2$ is still unsettled. The domain wall energy (e.g., positive or negative) between Pf and APf may significantly affect whether random Pf and APf domains are favored by the system, and such energy calculations have not been done yet. It is also important to have the tunability of disorders in the experiment to verify such a random Pf and APf domain percolation theory. Besides, whether the disordered $\kappa_{xy} = 3, 5/2$, and 2 phases can be identified with the known $K = 8$, PH-Pf and 113 FQH states in the clean limit should be further studied.

Below we comment final theoretical remarks and future directions:

(1) *Emergent symmetry vs spontaneous symmetry breaking*: We remark that in our study, as the disorder energy scale decreases/increases, the emergent symmetry is enhanced/reduced. This phenomenon is *opposite* to tuning energy scales in spontaneous symmetry breaking (SSB) systems. In the more familiar SSB systems, such as ferromagnets and superfluids, when the temperature scale decreases/increases, the symmetry is broken/restored. Another SSB example is quantum chromodynamics; when the temperature scale decreases/increases, the chiral symmetry and time reversal symmetry can be broken/restored.

(2) *Field theory and topological order data*: We refine the information in literatures in order to identify the fermionic spin topological quantum field theories (fTQFTs) for Pf/PH-Pf/APf states as well as 331, $K = 8$, 113 FQH states, and their bosonic TQFT (bTQFT) sectors. These data, including TQFTs and edge theories, are gathered together in Appendix A.[5] We find that their spin fTQFTs can be obtained as $U(1)_{\pm 8}$ Chern-Simons theory with additional $\nu \in \mathbb{Z}_8$-class TQFT, subject to a $\mathbb{Z}_2$-quotient constraint, which we may denote as $\frac{\mathrm{U}(1)_{\pm 8} \times (\nu \in \mathbb{Z}_8 \mathrm{TQFT})}{\mathbb{Z}_2}$, with other details in Appendix A. Our TQFT notations follow Refs. [62,63]. We also list down their modular $SL(2,\mathbb{Z})$ data $\mathcal{S}, \mathcal{T}$ matrices and chiral central charges c_- for bosonic sectors, which are modular theories in terms of category theory. The fTQFT however is premodular; one can extend our analysis to full fTQFTs based on the methods of Refs. [62,63]. Since global symmetries play important roles for these topological orders (TQFTs), in modern terminology, we provide the essential data to examine their symmetry enriched topologically ordered (SET) states. It will be worthwhile to revisit related Pf/PH-Pf/APf systems, considering the interplay of symmetries, in our framework, for a larger families of related SET states.

(3) *Nonperturbative gapping criteria analysis*: Based on the methods of Refs. [30,61], we provide nonperturbative gapping criteria on the domain walls of related quantum Hall systems. Even though certain interaction terms may be irrelevant in a perturbative RG sense, they can still affect domain wall properties at nonperturbative strong couplings. We are aware that the precise identifications of Pf/PH-Pf/APf and their domain walls require spin fTQFTs. We note that our methods in Appendices C and D are applicable to Abelian bosonic/fermionic TQFTs. For the convenience of bootstrapping the topological domain wall based on modular data, in Appendix E, we focus on the *non-Abelian* bTQFT sectors. At this moment, we believe that domain walls of bTQFT capture the major interesting effects. The further investigation of the domain wall theories of full fTQFTs is left for future work.

(4) *Abelian topological domain walls vs non-Abelian anyons*: In the main text, we mainly focus on the gapped double-semion domain wall sectors, which cause additional highly degenerate ground states in the Pf|APf percolation picture [Fig. 7(a)]. This is an astonishing long-range entanglement phenomenon. In contrast, the usual symmetry-breaking degeneracy scales as a product of individual degeneracy on each symmetry-breaking domain wall. As stressed in Ref. [30], the domain wall topological degeneracy contains nonlocal long-range entangled information between distinct domain walls (Appendix D/E).

[5] By spin TQFT (fTQFT), we mean that defining such TQFT requires a manifold with spin structures.

The double-semion sectors are purely Abelian topological orders. Even though many Abelian anyons (trapped by vortices or defect punctures) on a flat substrate has only a unique ground state (GSD = 1), the GSD of many topological domain walls of Abelian TQFT can still grow *exponentially*, respect to the number of anyon insertions, even on a flat substrate. The later GSD phenomenon from Abelian TQFT's topological domain walls is more similar to that of *non-Abelian* anyons instead.

(5) *Exotic non-Abelian topological domain walls*: In Appendices E 2 b and E 3, we include additional solutions of further exotic non-Abelian domain walls obtained from Pf|APf|Pf interface. The bosonic non-Abelian sector part of the interface can be described by tunneling data between two sets of Ising $\times SU(2)_2$ TQFTs. Ising and $SU(2)_2$ TQFTs consist of a set of anyon $\{1,\sigma_\nu,\psi_\nu\}$, labeled by $\nu = 1,3 \in \mathbb{Z}_8$, respectively, in terms of $2+1$D $\mathbb{Z}_8$-class TQFTs. For example, we find one intriguing set of interesting tunneling data of Pf|APf|Pf as $1\oplus\psi\psi_3 \leftrightarrow 1\oplus\psi\psi_3$, $\psi\oplus\psi_3 \leftrightarrow \psi\oplus\psi_3$, and $2\sigma\sigma_3 \leftrightarrow 2\sigma\sigma_3$. It is tempting to speculate their implications of junctionlike device. The tunneling data may be relevant to testable experimental settings.

ACKNOWLEDGMENTS

We thank Jie Wang and Michael Zaletel for helpful information and discussions. J.W. thanks Nathan Seiberg and Edward Witten for conversations and thanks collaborators for a previous collaboration on Ref. [63]. B.L. is supported by Princeton Center for Theoretical Science at Princeton University. J.W. gratefully acknowledges the support from Corning Glass Works Foundation Fellowship, NSF Grant PHY-1314311, and Institute for Advanced Study.

APPENDIX A: DATA OF QFT/TOPOLOGICAL ORDER: Pf/APf/PH-PFAFFIAN STATES

Here we first gather the data of topological orders and their topological quantum field theories (TQFTs) in Tables I, II, and III. Later we can use these data to determine all possible interfaces/domain walls. In Tables I and II's first column, we list down the underlying topological orders (Pfaffian/anti-Pfaffian/PH-Pfaffian and also $331/K = 8/113$ quantum Hall states) relevant for our work. In Tables I and II's second columns, we identify their bulk TQFTs and their gapless edge theories. By a symmetric bilinear K-matrix Abelian Chern-Simons theory (CS), we mean the action of (see more discussions in Appendix B 1):

$$S_{\text{bulk}}[a,A] = \frac{K_{IJ}}{4\pi}\int a_I da_J + \frac{q_I}{2\pi}\int A da_I. \quad \text{(A1)}$$

We denote q as the charge vector coupling to $U(1)$-background (electromagnetic) field A, and its transpose q^{T}, introduced later in Eq. (B25). The K-matrix CS with any diagonal entry of K_{II} as an odd integer is a fermionic TQFT (here as spin TQFT or simply fTQFT[6]). By a non-Abelian $U(2)_{k_2,k_1} \equiv (SU(2)_{k_2}\times U(1)_{k_1})/\mathbb{Z}_2$ Chern-Simons theory, we mean the action of:

$$S_{\text{bulk}} = \int \frac{k_2}{4\pi}\text{Tr}\left[bdb + \frac{2}{3}b^3\right] + \frac{k_1}{4\pi}ada, \quad \text{(A2)}$$

where b is an $SU(2)$ gauge field and a is a $U(1)$ gauge field, with a $\mathbb{Z}_2$-quotient constraint, following the notations of recent work [62,63]. The $\mathbb{Z}_2$ quotient is effectively obtained by gauging its $\mathbb{Z}_2$ 1-form global symmetry, which results in the modification of line operators (anyons) spectrum. In our case, this modification yields spin fTQFTs. The path integral is written as

$$Z[A] = \int [Da][Db]\exp(iS[a,b,A]),$$

where a,b are dynamical internal gauge fields that are summed over, while the A is the probed background field. For the identification of Pfaffian Moore-Read state as a fermionic spin fTQFT, we follow a remarkable Ref. [62].

For the gapless edge theories, we study the Majorana-Weyl modes and additional K-matrix multiplet chiral boson theories (see Appendix B). Indeed, we can rigorously show that, from Table I, $S_{\text{edge, A-Pfaff (i)}}$ can be transformed to $S_{\text{edge, A-Pfaff (ii)}}$ by the standard $GL(N,\mathbb{Z})$ field redefinition. Then we can rewrite the neutral ϕ_n chiral boson by fermionization to a complex fermion, then to two chiral Majorana-Weyl modes $\chi_{R,2}$ and $\chi_{R,3}$ (see Appendix D 1).

In Tables I and II's third columns, the c_L/c_R are left/right central charges. The q and t are the charge vectors [see Eq. (B25)]. The q_L/q_R are the charge coupling between internal gauge field a and external background electromagnetic A field. The σ_{xy} and κ_{xy} are quantum Hall (here only the Abelian K-matrix part is charged) and thermal Hall conductances:

$$\sigma_{xy} = q^{\mathrm{T}}K^{-1}q\left(\frac{e^2}{h}\right), \quad \kappa_{xy} = (c_L - c_R)\frac{\pi^2 k_B^2}{3h}T. \quad \text{(A3)}$$

In Tables I and II's fourth columns, we show ground state degeneracy (GSD) on a spatial torus T^2, where T^2 can have spin structures as T^2_{e} for the even and T^2_{o} for the odd [63,64]. The even spin structure T^2_{e} means that both S^1 1-cycle on T^2 has at least one in antiperiodic condition. The odd spin structure T^2_{o} means that both S^1 1-cycle on T^2 are both in periodic conditions. Following Refs. [63,64], the $\text{GSD}_{T^2} = \text{GSD}_{T^2_{\text{e}}|T^2_{\text{o}}}$ can be computed as the partition function $Z(T^2_{\text{e}}\times S^1_{\text{Iperiodic}})$ and $Z(T^2_{\text{o}}\times S^1_{\text{6periodic}})$, respectively. The GSD can have "b" for bosonic and "f" for fermionic sectors.

In Tables I and II's fifth columns, we summarize the pairing symmetry of composite fermions (CF) or composite Dirac fermions (CDF), in terms of Bardeen-Cooper-Schrieffer (BCS) mechanism, following a description in footnote 1 in the main text. In Table III, we show the modular SL(2,$\mathbb{Z}$) representation data, $\mathcal{S}^{xy}$ and $\mathcal{T}^{xy}$ matrices, in the good anyon quasiparticle basis (namely, in a good Wilson line basis), and again their chiral central charges c_-. Here we present their bosonic TQFT sectors. For the full spin fermionic TQFT, one can include the fermionic (f) sector $\{1,f\}$ with additional constraints. We can

[6]By spin TQFT or fTQFT, we mean the TQFT defined on *spin* manifolds. The underlying fTQFT can be viewed as the low energy physics theory emergent from a lattice model with fermionic degrees of freedom at high energy cutoff scale.

TABLE I. Data of Pf/PH-Pf/APf states. (Non-)Abelian Chern-Simons theories (CS) are identified. We provide both the fermionic spin TQFT (fTQFT) and the simplified bosonic TQFT (bTQFT) versions. Semion theory has a bulk action $U(1)_2$ CS as $\frac{2}{4\pi}\int ada$. The $\phi_s/\phi_{\bar{s}}$ stands for the chiral boson of semion/antisemion (with a level $k=2$). The ϕ_0 is the neutral chiral boson of a level $k=1$. The c_L/c_R and q_L/q_R are chiral central charges and charge couplings, $\mathrm{t}_{L/R} = K^{-1}q_{L/R}$ where K is given by a K-matrix CS. The σ_{xy},κ_{xy} are quantum/thermal Hall conductances.

State	2 + 1D TQFT description; 1 + 1D Edge modes	$(c_L, -c_R); c_-$ $(q_L,q_R); (\mathrm{t}_L,\mathrm{t}_R);$ σ_{xy} in $(\frac{e^2}{h})$; κ_{xy} in $(\frac{\pi^2 k_B^2}{3h}T)$.	GSD_{T^2}	Description: BCS pairing of fermions
(I) Pfaff (Moore-Read) $\kappa_{xy} = \frac{7}{2}$	fTQFT (spin): $\mathrm{U}(2)_{2,-8} \times \mathrm{U}(1)_1$ CS $\simeq (\mathrm{SU}(2)_2 \times \mathrm{U}(1)_{-8})/\mathbb{Z}_2 \times \mathrm{U}(1)_1$ CS $\simeq (\mathrm{U}(1)_8 \times \mathrm{Ising})/\mathbb{Z}_2$CS $\simeq$ Moore-Read state. bTQFT: Semion $\times$ Ising $+ \frac{q}{2\pi}\int Ada$. Anyons: $\{1,s\} \otimes \{1,\sigma,\psi\}$. $S_{\text{edge, Pf}} = \int_L dtdx \frac{2}{4\pi}\partial_x\phi_s(\partial_t\phi_s - v_1\partial_x\phi_s)$ $+\chi_L(i\partial_t - iv_L\partial_x)\chi_L + \frac{q}{2\pi}\epsilon^{\mu\nu}A_\mu\partial_\nu\phi_s|_{q=e1}$.	$(\frac{3}{2},0); \frac{3}{2}$ $(1+0,0)_q; (\frac{e}{2}\cdot 1 + 0,0)_{\mathrm{t}};$ $\sigma_{xy} = \frac{1}{2};$ $\kappa_{xy} = c_- + 2 = \frac{7}{2}$	6 (b+f)	Cooper pairs: $p+ip$ wave of CF $(d+id$ wave of CDF)
(II) PH-Pfaff $\kappa_{xy} = \frac{5}{2}$	fTQFT(spin): $(U(1)_8 \times \overline{\mathrm{Ising}})/\mathbb{Z}_2$ CS. bTQFT: Semion $\times$ $\overline{\mathrm{Ising}} + \frac{q}{2\pi}\int Ada$. Anyons: $\{1,s\} \otimes \{1,\bar{\sigma},\bar{\psi}\}$, $S_{\text{edge, PH-Pf}} = \int_L dtdx \frac{2}{4\pi}\partial_x\phi_s(\partial_t\phi_s - v_1\partial_x\phi_1)$ $+\int_R dtdx\chi_R(i\partial_t + iv_R\partial_x)\chi_R$ $+\int dtdx \frac{q}{2\pi}\epsilon^{\mu\nu}A_\mu\partial_\nu\phi_s|_{q=e1}$.	$(1,\frac{-1}{2}); \frac{1}{2}$ $(1,0)_q;$ $(\frac{e}{2}\cdot 1,0)_{\mathrm{t}};$ $\sigma_{xy} = \frac{1}{2};$ $\kappa_{xy} = c_- + 2 = \frac{5}{2}$.	6 (b+f)	Cooper pairs: $p-ip$ wave of CF (s wave of CDF)
(III) A-Pfaff $\kappa_{xy} = \frac{3}{2}$	fTQFT(spin): $U(2)_{-2,8}$ CS $\simeq (U(1)_8 \times \mathrm{SU}(2)_{-2})/\mathbb{Z}_2$ CS. bTQFT:Semion $\times$ $\mathrm{SU}(2)_{-2}$ CS $+ \frac{q}{2\pi}\int Ada$. Anyons:$\{1,s\} \otimes \{1,\bar{\sigma}_3,\bar{\psi}_3\}$, $S_{\text{edge, APf (i)}}$ $= \int dtdx \frac{1}{4\pi}\left(\begin{smallmatrix}1 & 0\\ 0 & -2\end{smallmatrix}\right)_{IJ}\partial_x\phi_I\partial_t\phi_J - V_{IJ}\partial_x\phi_I\partial_x\phi_J)$ $+\int dtdx \frac{q_I}{2\pi}\epsilon^{\mu\nu}A_\mu\partial_\nu\phi_I|_{q=e\left(\begin{smallmatrix}1\\1\end{smallmatrix}\right)}$ $+\int_R dtdx\chi_R(i\partial_t + iv_R\partial_x)\chi_R$, here $\phi_I \equiv (\phi_0,\phi_2)$. $\to S_{\text{edge, APf (ii)}}$ $= \int dtdx \frac{1}{4\pi}\left(\begin{smallmatrix}2 & 0\\ 0 & -1\end{smallmatrix}\right)_{IJ}\partial_x\phi_I\partial_t\phi_J - V_{IJ}\partial_x\phi_I\partial_x\phi_J)$ $+\int dtdx \frac{q_I}{2\pi}\epsilon^{\mu\nu}A_\mu\partial_\nu\phi_I|_{q=e\left(\begin{smallmatrix}1\\0\end{smallmatrix}\right)}$ $+\int_R dtdx\chi_R(i\partial_t + iv_R\partial_x)\chi_R$, here $\phi_I \equiv (\phi_s,\phi_n)$. $\to S_{\text{edge, APf (iii)}}$ $= \int_L dtdx \frac{2}{4\pi}\partial_x\phi_s(\partial_t\phi_s - v_s\partial_x\phi_s)$ $+\int dtdx \frac{q}{2\pi}\epsilon^{\mu\nu}A_\mu\partial_\nu\phi_s\ |_{q=e1}$ $+\int_R dtdx \sum_{j=1}^3 \chi_{Rj}(i\partial_t + iv_R\partial_x)\chi_{Rj}$.	$(1,\frac{-3}{2}); \frac{-1}{2}$ $(1,0)_q;$ $(e,\frac{e}{2}\cdot 1 + 0)_{\mathrm{t}}$ $\to (\frac{e}{2},0)_{\mathrm{t}};$ $\sigma_{xy} = \frac{1}{2};$ $\kappa_{xy} = c_- + 2 = \frac{3}{2}$.	6 (b+f)	Cooper pairs: $f-if$ wave of CF $(d-id$ wave of CDF)

consider the generators of mapping classes groups of T^2, the $SL(2,\mathbb{Z})$ modular data, permuting the spin structures on T^2, see Section 8 of Ref. [63].

In 2 + 1D, bosonic TQFT theory is modular in terms of category theory. Physically speaking, modular theory means that all nontrivial anyons have nontrivial (mutual) braiding statistics at least with respect to one other particle. Fermionic TQFT theory however is premodular. Fermionic theory has a fermion (electron) that has trivial (mutual) braiding statistics with respect to all other particles.

We write the rank-2 $\mathcal{S}^{xy}$ and $\mathcal{T}^{xy}$ matrices of semion theory in the $\{1,s\}$ basis (where s is the semion anyon). We write the rank-3 $\mathcal{S}^{xy}$ and $\mathcal{T}^{xy}$ matrices $\mathcal{V} \in \mathbb{Z}_8$ theory (here $\mathcal{V} = \pm 1, -3$) in $\{1,\sigma_\mathcal{V},\psi_\mathcal{V}\}$ basis. The $\sigma_\mathcal{V}$ is a non-Abelian Majorana zero mode also called σ anyon that is trapped at the core of π vortex ($\mathbb{Z}_2$-gauge flux line operator, with the vison at ends). The ψ is a Bogoliubov fermion solved from the Bogoliubov-de Gennes (BdG) equation. The fusion rules (denoted as a "$\times$" operation) of anyons follow:

$$1 \times s = s, \quad s \times s = 1. \tag{A4}$$

$$\sigma_\mathcal{V} \times \sigma_\mathcal{V} = 1 \oplus \psi_\mathcal{V}, \quad \sigma_\mathcal{V} \times \psi_\mathcal{V} = \sigma_\mathcal{V}, \quad \psi_\mathcal{V} \times \psi_\mathcal{V} = 1. \tag{A5}$$

TABLE II. The setup follows the same as Table I. Data of $331/K = 8/113$ quantum Hall states. Here $\mathcal{V} = 1,3 \in \mathbb{Z}_8$ state means some root of TQFT, where one can find other related bosonic/fermionic (spin-)TQFT data in Ref. [63].

State	2 + 1D TQFT description; 1 + 1D Edge modes	$(c_L,-c_R); c_-$ q_I; t_I; σ_{xy} in $(\frac{e^2}{h})$; κ_{xy} in $(\frac{\pi^2 k_B^2}{3h}T)$.	GSD_{T^2}	Description: BCS pairing of fermions
$K = 8$	$K = 8$ as a spin $U(1)_8$-Abelian CS + $\frac{q}{2\pi}\int A dA\,\vert_{q=2e}$; fTQFT may be denoted as $U(1)_8/\mathbb{Z}_2$-CS.	$(1,0); 0$ $(2)_q; (\frac{1}{4})_{\mathrm{t}}$	8	Cooper pairs: s wave of CF
$\kappa_{xy} = 3$	K-matrix multiplet chiral bosons Eq. (B2).	$\sigma_{xy} = \frac{1}{2}$; $\kappa_{xy} = c_- + 2 = 3$.		$(p + ip$ wave of CDF)
113-state	$K = \left(\begin{smallmatrix}1 & 3\\ 3 & 1\end{smallmatrix}\right)$-Abelian CS + $\frac{q}{2\pi}\int A dA\vert_{q=e\binom{1}{1}}$	$(1,-1); 0$		Cooper pairs:
	$\simeq \left(\begin{smallmatrix}1 & 0\\ 0 & -8\end{smallmatrix}\right)$-Abelian CS + $\frac{q}{2\pi}\int A dA\vert_{q=e\binom{1}{2}}$;	$(1,1)_q; (\frac{1}{4},\frac{1}{4})_{\mathrm{t}}$;	8	$d - id$ wave of CF
$\kappa_{xy} = 2$	K-matrix multiplet chiral bosons Eq. (B2).	$\sigma_{xy} = \frac{1}{2}$; $\kappa_{xy} = c_- + 2 = 2$.		$(p - ip$ wave of CDF)
	Other Root States (Not directly related to the $\nu = 5/2$ experiment and our phase diagram Fig. 2)			
331-state	$K = \left(\begin{smallmatrix}3 & 1\\ 1 & 3\end{smallmatrix}\right)$-Abelian CS+ $\frac{q}{2\pi}\int A dA\vert_{q=e\binom{1}{1}}$;	$(2,0); 0$		Cooper pairs:
$\kappa_{xy} = 4$	K-matrix multiplet chiral bosons Eq. (B2).	$(1,1)_q; (\frac{1}{4},\frac{1}{4})_{\mathrm{t}}$ $\sigma_{xy} = \frac{1}{2}$; $\kappa_{xy} = c_- + 2 = 4$.	8	$d + id$ wave of CF $(f + if$ wave of CDF)
$\mathcal{V} = 1$	Ising TQFT $\cong$ gauge$\mathbb{Z}_2^f$ of spin-Ising TQFT $\cong$ gauge $\mathbb{Z}_2^f$ of $p_x + ip_y$ superconductor $\cong$ $U(2)_{2,-4}$ CS $\cong$ $(SU(2)_2 \times U(1)_{-4})/\mathbb{Z}_2$ CS	$(\frac{1}{2},0); 0$ $(0,0); (0,0)$	3	
$\mathcal{V} = 3$	$SU(2)_2$ CS	$(\frac{3}{2},0); 0$ $(0,0); (0,0)$	3	

TABLE III. Here by the semion theory, we mean the action $S_{\mathrm{semion}} = \frac{2}{4\pi}\int a da$. The $\mathcal{S}^{xy}$ and $\mathcal{T}^{xy}$ are written in the bases of $\{1,\sigma_{\mathcal{V}},\psi_{\mathcal{V}}\}$, here $\mathcal{V} = 1,3 \in \mathbb{Z}_8$-class TQFTs. One can find other related $\mathcal{V} \in \mathbb{Z}_8$ fermionic (spin-)TQFT data in Ref. [63]. The chiral central charge $c_- \equiv c_L - c_R$ mod 8 is determined by the relation $(\mathcal{S}^{xy}\mathcal{T}^{xy})^3 = e^{2i\pi c_-/8}(\mathcal{S}^{xy})^2$.

State	2+1D TQFT description	$\mathcal{S}^{xy}$	$\mathcal{T}^{xy}$	c_-
$\mathcal{V} = 1$	Ising TQFT $\cong$ $U(2)_{2,-4}$ CS $\cong$ $(SU(2)_2 \times U(1)_{-4})/\mathbb{Z}_2$	$\frac{1}{2}\begin{pmatrix}1 & \sqrt{2} & 1\\ \sqrt{2} & 0 & -\sqrt{2}\\ 1 & -\sqrt{2} & 1\end{pmatrix}$	$\begin{pmatrix}1 & 0 & 0\\ 0 & e^{\frac{\pi i}{8}} & 0\\ 0 & 0 & -1\end{pmatrix}$	$\frac{1}{2}$
$\mathcal{V} = 3$	$SU(2)_2$ CS	$\frac{1}{2}\begin{pmatrix}1 & \sqrt{2} & 1\\ \sqrt{2} & 0 & -\sqrt{2}\\ 1 & -\sqrt{2} & 1\end{pmatrix}$	$\begin{pmatrix}1 & 0 & 0\\ 0 & e^{\frac{3\pi i}{8}} & 0\\ 0 & 0 & -1\end{pmatrix}$	$\frac{3}{2}$
Semion	$U(1)_2$ CS: $\frac{2}{4\pi}\int a da$	$\frac{1}{\sqrt{2}}\begin{pmatrix}1 & 1\\ 1 & -1\end{pmatrix}$	$\mathrm{diag}(1,\mathrm{i})$	1
Pfaff	fTQFT $\to$ simplified bTQFT: Semion $\times$ Ising, Anyons : $\{1,s\} \otimes \{1,\sigma,\psi\}$	$\begin{pmatrix}\frac{1}{\sqrt{2}} & \frac{1}{\sqrt{2}}\\ \frac{1}{\sqrt{2}} & -\frac{1}{\sqrt{2}}\end{pmatrix} \otimes \begin{pmatrix}\frac{1}{2} & \frac{1}{\sqrt{2}} & \frac{1}{2}\\ \frac{1}{\sqrt{2}} & 0 & -\frac{1}{\sqrt{2}}\\ \frac{1}{2} & -\frac{1}{\sqrt{2}} & \frac{1}{2}\end{pmatrix}$	$\mathrm{diag}(1,\mathrm{i}) \otimes \begin{pmatrix}1 & 0 & 0\\ 0 & e^{\frac{\pi i}{8}} & 0\\ 0 & 0 & -1\end{pmatrix}$	$\frac{1}{2}$
PH − Pfaff	fTQFT $\to$ simplified bTQFT: Semion $\times$ $\overline{\mathrm{Ising}}$, Anyons: $\{1,s\} \otimes \{1,\bar{\sigma},\bar{\psi}\}$	$\begin{pmatrix}\frac{1}{\sqrt{2}} & \frac{1}{\sqrt{2}}\\ \frac{1}{\sqrt{2}} & -\frac{1}{\sqrt{2}}\end{pmatrix} \otimes \begin{pmatrix}\frac{1}{2} & \frac{1}{\sqrt{2}} & \frac{1}{2}\\ \frac{1}{\sqrt{2}} & 0 & -\frac{1}{\sqrt{2}}\\ \frac{1}{2} & -\frac{1}{\sqrt{2}} & \frac{1}{2}\end{pmatrix}$	$\mathrm{diag}(1,\mathrm{i}) \otimes \begin{pmatrix}1 & 0 & 0\\ 0 & e^{-\frac{\pi i}{8}} & 0\\ 0 & 0 & -1\end{pmatrix}$	$\frac{-1}{2}$
A − Pfaff	fTQFT $\to$ simplified bTQFT : Semion $\times$ $SU(2)_{-2}$ CS, Anyons: $\{1,s\} \otimes \{1,\bar{\sigma}_3,\bar{\psi}_3\}$	$\begin{pmatrix}\frac{1}{\sqrt{2}} & \frac{1}{\sqrt{2}}\\ \frac{1}{\sqrt{2}} & -\frac{1}{\sqrt{2}}\end{pmatrix} \otimes \begin{pmatrix}\frac{1}{2} & \frac{1}{\sqrt{2}} & \frac{1}{2}\\ \frac{1}{\sqrt{2}} & 0 & -\frac{1}{\sqrt{2}}\\ \frac{1}{2} & -\frac{1}{\sqrt{2}} & \frac{1}{2}\end{pmatrix}$	$\mathrm{diag}(1,\mathrm{i}) \otimes \begin{pmatrix}1 & 0 & 0\\ 0 & e^{-\frac{3\pi i}{8}} & 0\\ 0 & 0 & -1\end{pmatrix}$	$\frac{-3}{2}$

See the renowned work [65] for an introduction to category theory and fusion/braiding properties of 2 + 1D TQFT. The classic developments root in Ref. [66].

APPENDIX B: CANONICAL QUANTIZATION OF K-MATRIX CHIRAL BOSON THEORY/LUTTINGER LIQUIDS

In Appendix A, we had describe the TQFT description of various Pf/PH-Pf/A-Pf states. When we only focus on the Abelian sectors, we can study them by simply using K-matrix Chern-Simons (CS) theory. In this section, we will focus on the Abelian CS and their edge K-matrix chiral boson theory/Luttinger liquids. Then we will use this info to demonstrate stability of gapless modes in the next Appendix C.

1. Bulk and boundary actions

The bulk action S_{bulk} of Abelian fractional quantum Hall state (described by an Abelian K-matrix CS theory) in the bulk $\mathcal{M} = \mathcal{M}^3$, and the boundary action S_∂ of its edge states (described by K-matrix chiral bosons/Luttinger liquids) on the boundary $\partial\mathcal{M} = \partial(\mathcal{M}^3) \equiv \Sigma^2$ are:

$$S_{\text{bulk}} = \frac{K_{IJ}}{4\pi}\int_{\mathcal{M}} dt\, d^2x\, \epsilon^{\mu\nu\rho} a_{I,\mu}\partial_\nu a_{J,\rho}, \tag{B1}$$

$$S_\partial = \frac{1}{4\pi}\int_{\partial\mathcal{M}} dt\, dx\, (K_{IJ}\partial_t\phi_I\partial_x\phi_J - V_{IJ}\partial_x\phi_I\partial_x\phi_J). \tag{B2}$$

Here K_{IJ} and V_{IJ} are symmetric integer bilinear $N \times N$ matrices; $a_{I,\mu}$ is the 1-form emergent gauge field's Ith component in the multiplet. The a gauge fields are an emergent degree of freedom after integrating out the bulk gapped matter fields. The above theories are RG fixed point TQFT in the bulk and the gapless theory on the edge. The V_{IJ} is positive definite for the *potential energy* like term to be bounded from below [see Eq. (B14)]. Each mode has individual chiral central charge $|c_L - c_R| = 1$. The number of left moving modes subtracting the number of right moving modes, say the total chiral central charge

$$c_- \equiv c_L - c_R = \text{signature}\,(K),$$

is the signature of K matrix (numbers of positive eigenvalues subtracts negative eigenvalues). We will allow to add interactions later in Appendix C to explore the gap edge/domain wall:

$$S_{\partial,\text{interaction}} = \int_{\partial\mathcal{M}} dt\, dx \sum_{\text{a}} g_{\text{a}} \cos(\ell_{\text{a},I}\cdot\phi_I), \tag{B3}$$

where a are different components. However, below we like to first canonical quantize the gapless edge theory Eq. (B2) in Sec. B 2.

2. Canonical Quantization of multiplet Chiral Boson Field Theory

In the literature, there are vast but no generic treatments on canonical quantization of multiplets-chiral boson theory. So we aim to be self-contained; we start from scratch. Below we will be pedagogical for our convention and definition.

The time-independent mode expansion of $\phi_I(x)$ on a *compact* circle $x \in [0, L)$ that we construct is:

$$\phi_I(x) \equiv \phi_{0I} + K^{-1}_{IJ} P_{\phi_J}\frac{2\pi}{L}x + i\sum_{n\neq 0}\frac{1}{n}\alpha_{I,n}e^{-inx\frac{2\pi}{L}}. \tag{B4}$$

We write zero mode part as ϕ_{0I}. The conjugate winding momentum is P_{ϕ_I}. All of ϕ_{0I}, P_{ϕ_J}, and nonzero mode part, Fourier modes $\alpha_{I,n}$, should regard as operators (instead of complex numbers). Our canonical quantization is performed by imposing following commutation relations. The canonical conjugation relation of zero mode and winding momentum is

$$[\phi_{0I}, P_{\phi_J}] = i\delta_{IJ}. \tag{B5}$$

The nonzero Fourier modes part satisfies a generalized Kac-Moody algebra:

$$[\alpha_{I,n}, \alpha_{J,m}] = nK^{-1}_{IJ}\delta_{n,-m}. \tag{B6}$$

The conjugate momentum field $\Pi_I(x)$ of $\phi_I(x)$ is:

$$\begin{aligned}\Pi_I(x) &= \frac{\delta L}{\delta(\partial_t\phi_I)} = \frac{1}{4\pi}K_{IJ}\partial_x\phi_J \\ &= \frac{1}{4\pi}\frac{2\pi}{L}\left(P_{\phi_I} + \sum_{n\neq 0}K_{IJ}\alpha_{J,n}e^{-inx\frac{2\pi}{L}}\right).\end{aligned} \tag{B7}$$

We can check consistently the canonical conjugation relation of operators $\phi_I(x_1)$ and $\Pi_J(x_2)$:

$$\begin{aligned}[\phi_I(x_1), \Pi_J(x_2)] &= \frac{1}{4\pi}\frac{2\pi}{L}i\delta_{IJ}\left(1 + \sum_{n\neq 0}e^{-in(x_1-x_2)\frac{2\pi}{L}}\right) \\ &= \frac{1}{4\pi}\frac{2\pi}{L}i\delta_{IJ}\sum_{n\in\mathbb{Z}}e^{-in(x_1-x_2)\frac{2\pi}{L}} \\ &= \frac{1}{2}i\delta_{IJ}\delta(x_1 - x_2),\end{aligned} \tag{B8}$$

where we derive and apply some Fourier transformation formulas.[7] We comment that the factor is $\frac{1}{2}$ instead of 1 in

[7] We derive Fourier transformation formulas:

$$\frac{1}{2\pi}\int_0^{2\pi} e^{i(m-n)\varphi}d\varphi = \delta_{m,n}, \tag{B9}$$

$$\frac{1}{2\pi}\int_0^{L} e^{i\frac{2\pi}{L}nx}dx = \frac{L}{2\pi}\delta_{n,0}, \tag{B10}$$

$$\frac{1}{2\pi}\int_{-\infty}^{\infty} e^{ikx}dx = \delta(k), \tag{B11}$$

$$\sum_{n\in\mathbb{Z}} e^{-in(x_1-x_2)\frac{2\pi}{L}} = L\delta(x_1 - x_2). \tag{B12}$$

The first line is proved by complex analysis:

$$\delta_{m,n} = \frac{1}{2\pi i}\oint_{|z|=1} z^{m-n-1}dz = \frac{1}{2\pi}\int_0^{2\pi} e^{i(m-n)\varphi}d\varphi.$$

The second line is proved by replacing the first line to:

$$\delta_{m,n} = \frac{1}{2\pi}\int_0^{2\pi} e^{i(m-n)\varphi}d\varphi = \frac{1}{L}\int_{x=0}^{x=L} e^{i\frac{2\pi(m-n)}{L}x}dx,$$

$\frac{1}{2}i\delta_{IJ}\delta(x_1-x_2)$, due to that we have each mode as chiral modes. If we have two modes together with the combined left and right nonchiral modes, the sum of two modes gives $i\delta_{IJ}\delta(x_1-x_2)$.

a. Equation of motion

The equation of motion (E.O.M) of Eq. (B2) is

$$\begin{aligned}&\frac{\partial L}{\partial(\phi_I)}-\partial_\mu\left(\frac{\partial L}{\partial(\partial_\mu\phi_I)}\right)\\&=\frac{1}{4\pi}(-2)\partial_x(K_{IJ}\partial_t\phi_J-V_{IJ}\partial_x\phi_J)=0\\&\Rightarrow K_{IJ}\partial_t\phi_J-V_{IJ}\partial_x\phi_J\\&=f(t),\quad\text{and }(K_{IJ}\partial_t\rho_J-V_{IJ}\partial_x\rho_J)=0.\end{aligned}\tag{B13}$$

Here $\rho_J\equiv\frac{1}{2\pi}\partial_x\phi_J(x)$ can be regarded as the density field. The V_{IJ} is a positive definite matrix, so the sign of eigenvalues of K_{IJ} determines the left or right moving modes. Positive eigenvalues are left (L) moving, and negative eigenvalues are right (R) moving. One simple trick to see this L/R moving is based on the E.O.M. of the forms: $(\partial_t-v\partial_x)\phi_L(vt+x)$ and $(\partial_t+v\partial_x)\phi_R(vt-x)$, then simply drawing their wave packets in the (t,x) plane.

b. Hamiltonian

The time-independent Hamiltonian is:

$$\begin{aligned}H&=\int_0^L dx\left[\Pi^I\frac{\partial L}{\partial(\partial_t\phi_I)}-L\right]=\int_0^L dx\ [V_{IJ}\partial_x\phi_I\partial_x\phi_J]\\&=\frac{1}{4\pi}\frac{(2\pi)^2}{L}\left[V_{IJ}K^{-1}_{Il1}K^{-1}_{Jl2}P_{\phi_{l1}}P_{\phi_{l2}}+\sum_{n\neq0}V_{IJ}\alpha_{I,n}\alpha_{J,-n}\right].\end{aligned}\tag{B14}$$

Notice that the Hamiltonian only depends on the winding mode parts (P_ϕ), and the positive-definite velocity matrix (V_{IJ}) gives rise to a potential like term for Fourier modes ($\alpha_{I,n}$).

---

with $x\equiv\frac{L}{2\pi}\varphi$, $k\equiv\frac{2\pi(m-n)}{L}$, so

$$\delta_{m,n}=\frac{1}{2\pi}\int_{-\pi}^{\pi}e^{i(m-n)\varphi}d\varphi=\frac{1}{L}\int_{x=-\pi\frac{L}{2\pi}}^{x=\pi\frac{L}{2\pi}}e^{i\frac{2\pi(m-n)}{L}x}dx.$$

The third line is proved by taking $L\to\infty$:

$$\frac{1}{2\pi}\int_{-\infty}^{\infty}e^{ikx}dx=\lim_{L\to\infty}\frac{L}{2\pi}\delta_{m,n}=\delta\left(\frac{2\pi}{L}(m-n)\right)=\delta(k).$$

The fourth line is shown by relating a sum to a continuous limit (with $k_n=\frac{2\pi n}{L}$):

$$\begin{aligned}\sum_{n\in\mathbb{Z}}e^{-in(x_1-x_2)\frac{2\pi}{L}}&=\sum_{n\in\mathbb{Z}}e^{-ik_n(x_1-x_2)}(k_{n+1}-k_n)\frac{L}{2\pi}\\&\to\int e^{-ik(x_1-x_2)}dk\frac{L}{2\pi}=L\delta(x_1-x_2).\end{aligned}$$

c. Time-in/dependent (Schrödinger/Heisenberg picture) mode expansion

The mode expansion we use is a time-independent operator (Schrödinger picture) $\phi_I(x)$ in Eq. (B4); we now check whether the time-dependent operator (Heisenberg picture) $\phi_I(x,t)$ satisfies the E.O.M. and whether the time-dependent part show the left, right moving modes explicitly.

One quick method to calculate $\phi_I(x,t)$ is going reversely to find the constraints from E.O.M. For example, writing:

$$\begin{aligned}\phi_I(x,t)=\phi_{0I}+K^{-1}_{IJ}P_{\phi_J}\frac{2\pi}{L}x+\tilde{V}_{Il}P_{\phi_l}\frac{2\pi}{L}t\\+i\sum_{n\neq0}\frac{1}{n}(\alpha_{l',n}e^{-int\frac{2\pi}{L}M_{Il'}}e^{-inx\frac{2\pi}{L}}).\end{aligned}\tag{B15}$$

Check that $K_{IJ}\partial_t\phi_J-V_{IJ}\partial_x\phi_J=0$ imposes: $\tilde{V}_{Il}=K^{-1}_{II'}V_{I'J'}K^{-1}_{J'l}$ and $M_{Il'}=K^{-1}_{Il}V_{ll'}$.

The alternative standard method, we can calculate $\phi_I(x,t)=e^{iHt}\phi_I(x)e^{-iHt}$. We find:

$$[H,\phi_{0I}]=\frac{1}{4\pi}2\frac{(2\pi)^2}{L}(-i)K^{-1}_{II'}V_{I'J'}K^{-1}_{J'l}P_{\phi_l},\tag{B16}$$

$$[H,P_{\phi_I}]=0,\tag{B17}$$

$$\begin{aligned}[H,\alpha_{I,n}]&=\frac{1}{4\pi}2\frac{(2\pi)^2}{L}(-n)K^{-1}_{J'I}V_{I'J'}\alpha_{I',n}\\&=\frac{1}{4\pi}2\frac{(2\pi)^2}{L}(-n)K^{-1}_{IJ}V_{JI'}\alpha_{I',n}.\end{aligned}\tag{B18}$$

Plug in we derive the exactly consistent result above:

$$\phi_I(x,t)=e^{iHt}\phi_I(x)e^{-iHt}=\text{Eq. (B15)}.\tag{B19}$$

This concludes our canonical quantization of the gapless multiplet chiral boson theory.

3. Global symmetry and charge vector

Additionally we can consider a charge vector q_I coupling to an external (e.g., electromagnetic) field A_μ of $U(1)$ global symmetry, by adding a coupling term $A_\mu q_I J^\mu_I$ with a symmetry current $q_I J^\mu_I=\frac{q_I}{2\pi}\epsilon^{\mu\nu\rho}\partial_\nu a_{I,\rho}$ as

$$\int dtd^2x\ \frac{q_I}{2\pi}\ \epsilon^{\mu\nu\rho}A_\mu\partial_\nu a_{I,\rho}\tag{B20}$$

into the S_{bulk} of Eq. (B1). From reading the E.O.M. of "Eq. (B1) plus the external probe Eq. (B25),"

$$e\,q_J\,J^\mu_J=-q_I\frac{e^2}{h}K^{-1}_{IJ}q_J\epsilon^{\mu\nu\rho}\partial_\nu A_\rho,\tag{B21}$$

we can derive that the Hall conductance $\sigma_{xy}=q^{\mathrm{T}}K^{-1}q(\frac{e^2}{h})$ as Eq. (A3) from $J_x\propto\sigma_{xy}E_y$. Meanwhile on the boundary, we can add the following coupling term

$$\int dtdx\ \frac{q_I}{2\pi}\ \epsilon^{\mu\nu}A_\mu\partial_\nu\phi_I,\tag{B22}$$

with a boundary symmetry current $q_I j^\mu_I=\frac{q_I}{2\pi}\epsilon^{\mu\nu}\partial_\nu\phi_I$ into the S_∂ of Eq. (B2). The symmetry operator on boundary is generated by the symmetry current, thus

$\mathrm{U}_{\rm sym} = \exp(i\,\theta\,\frac{q_I}{2\pi}\int \partial_x\phi_I)$, with any $U(1)$ angle θ. The induced symmetry transformation acts on ϕ_I as:

$$(\mathrm{U}_{\rm sym})\phi_I(\mathrm{U}_{\rm sym})^{-1} = \phi_I - i\theta\int dx\,\frac{q_I}{2\pi}[\phi_I,\partial_x\phi_I] = \phi_I + \theta(K^{-1})_{Il}q_l \equiv \phi_I + \theta \mathrm{t}_I; \quad \text{(B23)}$$

here we use the canonical commutation relation Eq. (B8) as $[\phi_I,\partial_x\phi_I] = 2\pi i\,(K^{-1})_{Il}$. A different *charge vector* t_I is commonly defined by a K inverse with the original charge vector q vector:

$$\mathrm{t}_I \equiv (K^{-1})_{Il}q_l. \quad \text{(B24)}$$

Given any internal line operator $\exp(i\ell_I\int a_I)$ in the bulk, we can compute its associated charge,

$$q_I K^{-1}_{IJ}\ell_J = \mathrm{t}_J\ell_J, \quad \text{(B25)}$$

viewed as the charge of anyon (living on the end of an open line operator), generated by $U(1)$ symmetry operator $U_{\rm sym}$. Then there is also a charge

$$q_I Q_I = q_I\frac{1}{2\pi}\int_0^L \partial_x\Phi_I dx = q_I K^{-1}_{IJ}P_{\phi_J} \quad \text{(B26)}$$

associated to each edge mode ϕ_I on the boundary.

4. $GL(N,\mathbb{Z})$ or $SL(N,\mathbb{Z})$ field redefinition

We can implement a field redefinition under $U \in \mathrm{GL}(N,\mathbb{Z})$ [or $U \in \mathrm{SL}(N,\mathbb{Z})$] such that the original and new quantities are related

$$\vec{\tilde\phi} = U\vec\phi, \quad \tilde K = U^{\mathrm{T}^{-1}}KU^{-1}, \quad \tilde q^{\mathrm{T}} = q^{\mathrm{T}}U^{-1}, \quad \text{(B27)}$$

with the vector $\vec\phi$ abbreviates ϕ_I. Several quantities in the action are invariant, e.g.,

$$\phi_I^{\mathrm{T}}K_{IJ}\phi_J = (\phi^{\mathrm{T}}U^{\mathrm{T}})(U^{\mathrm{T}^{-1}}KU^{-1})(U\phi) = \tilde\phi_I^{\mathrm{T}}\tilde K_{IJ}\tilde\phi_J.$$
$$q^{\mathrm{T}}\phi = (q^{\mathrm{T}}U^{-1})(U\phi) = \tilde q^{\mathrm{T}}\tilde\phi. \quad \text{(B28)}$$

This method will be used in Appendix D.

APPENDIX C: GAPPED BOUNDARY, TOPOLOGICAL STABILITY, AND LAGRANGIAN SUBGROUP

Now we like to include Eq. (B3)'s interaction, the sine-Gordon cosine term $S_{\partial,\rm interaction} = \int_{\partial\mathcal{M}} dt\ dx\ \sum_{\rm a} g_{\rm a}\cos(\ell_{{\rm a},I}\cdot\phi_I)$ into the free-quadratic action of gapless theory Eq. (B2). One well-known issue is under what criteria the gapless edge modes can be gapped under $S_{\partial,\rm interaction}$. Here we will focus on the *nonperturbative* analysis; consider the full interacting action:

$$S_{\rm edge} = S_\partial + S_{\partial,\rm interaction} = \frac{1}{4\pi}\int_{\partial\mathcal{M}} dt\,dx\,(K_{IJ}\partial_t\phi_I\partial_x\phi_J - V_{IJ}\partial_x\phi_I\partial_x\phi_J) + \int_{\partial\mathcal{M}} dt\,dx\sum_{\rm a} g_{\rm a}\cos(\ell_{{\rm a},I}\cdot\phi_I). \quad \text{(C1)}$$

By *nonperturbative*, we mean that without limiting to *relevant* operators in the RG sense, the *irrelevant* term at a strong coupling g at the high-energy ultraviolet (UV) lattice scale, can still *gap* the gapless modes. The classic analysis is first done by Ref. [46], hence the name of Haldane stability. Our analysis follows a more modern view derived in Ref. [30] (See also a closely related work [31]). In a more mathematical term, to obtain the topological gapped boundary, one needs to implement a *Lagrangian subgroup* structure [67] at the field theory.

Below we like to derive the stability of topological boundary condition in a self-contained consistent modern view, using both field theory and condensed matter intuition. To this end, first we recall that the Abelian mutual/self statistics of Abelian anyons, of the internal line operator $\exp(i\ell_{{\rm a},I}\int a_I)$ of the bulk action Eq. (B1), is given by

$$\exp[i\theta_{\rm mutual}] = \exp[i\theta_{\rm ab}] = \exp\left[i\,2\pi\,\ell_{{\rm a},I}K^{-1}_{IJ}\ell_{{\rm b},J}\right],$$
$$\exp[i\theta_{\rm self}] = \exp\left[i\frac{\theta_{\rm aa}}{2}\right] = \exp\left[i\pi\,\ell_{{\rm a},I}K^{-1}_{IJ}\ell_{{\rm a},J}\right]. \quad \text{(C2)}$$

This can be easily derived as the path integral of Hopf link of two line operators labeled by $\ell_{\rm a}/\ell_{\rm b}$ with proper normalization, see Sec. III of Ref. [63] for a derivation. In terms of a recent description in Ref. [64], we can view that the topological boundary condition on the edge $\partial\mathcal{M}$ sets the boundary gauge degrees of freedom vanishes,

$$\ell_{{\rm a},I}a_I|_{\partial\mathcal{M}} = 0. \quad \text{(C3)}$$

The boson modes ϕ_I, originally related by the gauge transformation $a_I \to a_I + d\lambda_I$ and $\phi_I \to \phi_I - \lambda_I$, now may be able to condense on the boundary,

$$\langle\exp[i(\ell_I\cdot\phi_I)]\rangle|_{\partial\mathcal{M}} \neq 0,$$
$$\text{more precisely, indeed } \left\langle\exp\left[i\left(\frac{\ell_I}{|\gcd(\ell_I)|}\cdot\phi_I\right)\right]\right\rangle\Big|_{\partial\mathcal{M}} \neq 0, \quad \text{(C4)}$$

where $\gcd(\ell_I) \equiv \gcd(\ell_1,\ell_2,\ldots,\ell_N)$ is the greatest common divisor (gcd) of all components of ℓ. This condensation is precisely triggered by the cosine term at strong coupling

$$g\int_{\partial\mathcal{M}} dt\,dx\,\cos(\ell_I\cdot\phi_I). \quad \text{(C5)}$$

Moreover, the set of *condensed anyons* should be generated by a subset (not necessarily the full set) of

$$\ell'_I = n\frac{\ell_I}{|\gcd(\ell_I)|}, \quad n \in \mathbb{Z}_{|\gcd(\ell_I)|}. \quad \text{(C6)}$$

We say that *anyons* labeled by ℓ'_I corresponds to the internal line operator $\exp(i\ell'_{{\rm a},I}\int a_I)$ in the bulk; the anyons living on the open ends of this line operator that can have open ends on the boundary as Eq. (C3). With the above information, below we summarize the criteria in Ref. [30] answering "*which set of interaction terms and consequential condensations can obtain a stable gapped boundary?*"

(1) Trivial self statistics: $\ell'_{{\rm a},I}K^{-1}_{IJ}\ell'_{{\rm a},J} \in 2\mathbb{Z}$ even integers for bosonic systems, or in $\mathbb{Z}$ odd integers for fermionic systems. This means that the self-statistics of ℓ'_a line operator is bosonic/fermionic, with $\theta_{\rm self}$ a multiple 2π or π phase.

(2) Trivial mutual statistics: $\ell'_{{\rm a},I}K^{-1}_{IJ}\ell'_{{\rm b},J} \in \mathbb{Z}$ integers. Anyons labeled by $\ell'_{\rm a}$ braid around $\ell'_{\rm b}$ must yield a trivial mutual bosonic statistical phase. In a spacetime picture, the

line operator labeled by $\ell'_{\rm a}$ linked with $\ell'_{\rm b}$ yields a path integral without any complex phase.

(3) Nonfractionalized interaction terms: The ℓ in $\cos(\ell_I \cdot \phi_I)$ term must be excitations of nonfractionalized degrees of freedom (e.g., electrons or local bosons). In terms of Chern-Simons K matrix, the column/row vector of K represents a nonfractionalized operator [e.g., $\exp(i \sum_J \mathrm{c}_J K_{IJ} \int a_I)$ is a nonfractionalized line operator], thus

$$\ell_I = \sum_J \mathrm{c}_J K_{IJ}, \quad \mathrm{c}_J \in \mathbb{Z}. \tag{C7}$$

This criterion imposes integral charges for the bulk object's charge Eq. (B25) as well as boundary charge Eq. (B26) on $\ell_I \phi_I$ edge mode.

In contrast, the anyonic operator ℓ' in Eq. (C6) takes integer values. The ℓ' is *not* a linear combination of column vectors of K matrix, thus fractional with respect to K.

(4) Completeness: We find all the condensed anyon $\{\ell'_{\rm a}, \ell'_{\rm b}, \dots\}$ as a complete set, by including every possible term $\ell'_{\rm c}$ that has trivial self braiding statistics (criterion 1) and trivial mutually braiding statistics (criterion 2) respect to all the elements $\{\ell'_{\rm a}, \ell'_{\rm b}, \dots\}$.

(5) Nonchiral: To fully gap out the gapless modes, we need that the chiral central charge $c_L - c_R = 0$, thus Eq. (A3)'s thermal Hall conductance requires $\kappa_{xy} = 0$.

The detailed derivation of the above criteria can be found in Ref. [30]. Here we only like to remark some physics intuitions behind.

(i) First, from the edge theory, in order to pin down the zero mode at strong coupling, we require

$$\begin{aligned} & g_{\rm a} \int_0^L dx \ \cos(\ell_{{\rm a},I} \cdot \phi_I) \\ & \to \int_0^L dx \ \cos\left(\ell_{{\rm a},I} \cdot \left(\phi_{0I} + K^{-1}_{IJ} P_{\phi_J} \frac{2\pi}{L} x\right)\right) \\ & = g_{\rm a} L \ \cos(\ell_{{\rm a},I} \cdot \phi_{0I}) \, \delta_{(\ell_{{\rm a},I} \cdot K^{-1}_{IJ} P_{\phi_J}, 0)}. \end{aligned}$$

The approximation is firstly due to a strong coupling thus focusing on zero/winding modes to determine the lowest energy spectrum. The second equality holds, if $\ell_{{\rm a},I}$ has trivial statistics (criteria 1 and 2, but obviously to see if it satisfies the *null* condition), see Ref. [30], we can pin down zero modes by strong coupling $g_{\rm a} \cos(\ell_{{\rm a},I} \cdot \phi_{0I})$ provided $\ell_{{\rm a},I} \cdot K^{-1}_{IJ} P_{\phi_I} = 0$.

(ii) Second, from the bulk theory, the trivial statistics $\exp[i\theta_{\rm mutual}] = \exp[i\theta_{\rm self}] = 1$ helps to stabilize the path integral Z, thus helping to achieving the quantum stability for gapped phases without unwanted fluctuations causing gapless modes.

(iii) Third, the nonfractionalized interaction term for ℓ (criterion 3) is important to calculate the precise bulk and boundary/domain wall GSD [30], later shown in Appendix D.

We comment that the similar/*simplified* criteria are derived but formulated in terms of a Lagrangian subgroup in Ref. [31]. These results [30,31] only work for Abelian topological order/TQFT. Later we will implement the generalized criteria for the non-Abelian case [61] in Appendix E.

In addition, if we like the interaction terms to preserve a symmetry [e.g. $U(1)$ charge conservation in the main text, in Sec. IV], say the boson/fermion charge symmetry as $\phi_I \to \phi_I + K^{-1}_{IJ} q_J \theta = \phi_I + t_I \theta$ and $\psi_I \to \psi_I e^{i K^{-1}_{IJ} q_J \theta} = \psi_I e^{i t_I \theta}$, then we require that $\cos(\ell_I \cdot \phi_I) = \cos(\ell_I \cdot (\phi_I + K^{-1}_{IJ} q_J \theta))$. For a $U(1)$-charge symmetry, this requires that $\ell_I K^{-1}_{IJ} q_J = 0$.

APPENDIX D: DERIVATIONS: ZERO MODES AND GSD COUNTING WITH GAPPED DOMAIN WALLS

1. Gapped sector of Pf|APf domain wall

We like to implement the gapping criteria Appendix C to our domain wall theory on Pf|APf with data summarized in Appendix A. The only sectors of edge modes that are Abelian are the chiral boson (e.g., semion) sectors. Here we follow the treatment of gapping interaction terms of Ref. [30].

Based on Table I, we can study the domain wall of Pf|APf, by considering the actions $S_{\text{edge, Pf}} + \bar{S}_{\text{edge, APf}}$. Here we write $\bar{S}$ meaning that reversing the chirality of edge modes in S is due to the folding/orientation at the interface. Starting from Table I's $S_{\text{edge, Pf}} + \bar{S}_{\text{edge, APf (i)}}$, denoting its K-matrix data as $K_{\rm (i)}$, we can find an $SL(3,\mathbb{Z})$ matrix $U_{\rm (i \leftrightarrow ii)}$ transforming the theory to Table I's $S_{\text{edge, Pf}} + \bar{S}_{\text{edge, APf (ii)}}$, based on Eq. (B27)/(B28):

$$\begin{aligned} K_{\rm (i)} &= \begin{pmatrix} 2 & 0 & 0 \\ 0 & -1 & 0 \\ 0 & 0 & 2 \end{pmatrix}, \quad \begin{pmatrix} \phi_1 \\ \phi_0 \\ \phi_2 \end{pmatrix}, \quad q = \begin{pmatrix} 1 \\ 1 \\ 1 \end{pmatrix} \overset{U_{\rm (i \leftrightarrow ii)}}{\Longleftrightarrow} K_{\rm (ii)} \\ &= \begin{pmatrix} 2 & 0 & 0 \\ 0 & -2 & 0 \\ 0 & 0 & 1 \end{pmatrix}, \quad \begin{pmatrix} \phi_s \\ \phi_{\bar{s}} \\ \phi_n \end{pmatrix}, \quad q = \begin{pmatrix} 1 \\ 1 \\ 0 \end{pmatrix}, \\ U_{\rm (i \leftrightarrow ii)} &= \begin{pmatrix} 1 & 0 & 0 \\ 0 & 1 & 1 \\ 0 & 1 & 2 \end{pmatrix}, \quad U^{-1}_{\rm (i \leftrightarrow ii)} = \begin{pmatrix} 1 & 0 & 0 \\ 0 & 2 & -1 \\ 0 & -1 & 1 \end{pmatrix}. \end{aligned} \tag{D1}$$

After rewriting the neutral chiral boson ϕ_n to two chiral Majorana-Weyl modes, we obtain Table I's $S_{\text{edge, Pf}} + \bar{S}_{\text{edge, APf (iii)}}$. Since the net chiral central charge has $c_L - c_R = 2$ (e.g., four chiral Majorana-Weyl modes), they cannot be fully gapped, due to violating the criterion 5 in Appendix C. However the double semion (DS) sectors within $K_{\rm (ii)}$, with $K_{\rm DS} = \left(\begin{smallmatrix} 2 & 0 \\ 0 & -2 \end{smallmatrix}\right)$ and boson modes $\left(\begin{smallmatrix} \phi_s \\ \phi_{\bar{s}} \end{smallmatrix}\right)$ can be fully gapped.[8] The criterion 5 holds because $c_L - c_R = 1 - 1 = 0$ for the double semion's $K_{\rm DS}$. The criteria 1, 2, and 4 say that we should condense a set of anyons labeled by ℓ' as

$$\begin{aligned} \{\ell'\} &= \{(1,1),(1,-1),(2,2),(2,-2),(2,0),(0,2), \dots\} \\ &= \{(1,1)\zeta,(1,-1)\zeta' \mid \zeta,\zeta' \in \mathbb{Z} \dots\}. \end{aligned} \tag{D2}$$

We say $\ell' = (1,1)$ implies the condensation of double semions $s\bar{s}$ on the domain wall, while other terms are related by only nonfractionalized objects. (Namely, it has a $\mathbb{Z}_2$-fusion rule, thus it has mod 2 invariant.) The criterion 3 says that $S_{\partial,\text{interaction}}$

[8] Indeed, this is the only Abelian sector that can be fully gapped. However, using the gapping criteria for more exotic non-Abelian in Appendix E, we can explore other types of domain wall.

in Eq. (C1) requires:

$$g \int_{\text{domain}} dt\, dx \cos(2(\phi_s + \phi_{\bar{s}})) + \cdots . \tag{D3}$$

In principle, naively the … terms can include $g' \int_{\text{domain}} dt\, dx \cos(2(\phi_s - \phi_{\bar{s}})) + g_s \int dt\, dx \cos(2\phi_s) + g_{\bar{s}} \int dt\, dx \cos(2\phi_{\bar{s}})$.[9] We remark that, in the context of Sec. IV, under the $U(1)$-charge conservation constraint, only this Eq. (21), the $\cos(2(\phi_s + \phi_{\bar{s}}))$ term is allowed. But we will see that these additional terms, on one hand, do not affect the counting of GSD contributed from zero/winding modes (see Fig. 8), and on the other hand, they are *not required* to fully gap out the edge modes as long as we have Eq. (D3). As noted in Ref. [30], we only require a half of the rank of K, say a rank(K)/2 (here $2/2 = 1$) number of interaction term(s) to fully gap the nonchiral (Abelian) edge modes. Equation (D3) is the single required term, satisfying all gapping criteria in Appendix C.

2. Zero modes and GSD counting for percolating Pf|APf domain walls: Double-Semion sector

Now we count the ground state degeneracy (GSD) for a number of n Pf|APf domain walls in the percolation picture. Since the Pfaffian-anti-Pfaffian domain wall has the edge states of $\mathbb{Z}_2$-double-semion (twisted $\mathbb{Z}_2$-gauge theory), below we focus on demonstrating counting the GSD and zero modes for such a gapped theory. The zero modes are topological robust and are nonlocal long-ranged entangled (LRE) phenomenon. On the space without nontrivial cycle [here the trivial homology class $H_1(\mathcal{M},\mathbb{Z}_2)$], such as a spatial sphere S^2 or a flat substrate experimental sample $\mathbb{R}^2$, we like to show that n-double-semion domain walls contribute additional 2^{n-1} ground states. We can say that there is

$$\text{GSD}_{\mathcal{M}^2_{\text{flat space}}} = \dim \mathcal{H}_{\mathcal{M}^2_{\text{flat space}}} = \left| Z_{\mathcal{M}^2_{\text{flat space}} \times S^1_{\text{time}}} \right| = 2^{n-1}, \tag{D4}$$

simply on the flat space $\mathcal{M}^2_{\text{flat space}}$. Here Z is the path integral of the whole system (including the bulk and domain walls/boundaries), while the $\mathcal{M}^2_{\text{flat space}}$ is the space with domain walls/boundaries. Of course, in the Pfaffian-anti-Pfaffian domain wall in a percolation picture, there are *additional four gapless neutral chiral Majorana-Weyl modes* ($|c_L - c_R| = 2$) on each domain wall. However, due to finite size effect of volume V, the energy split Δ_E of topological zero modes are exponentially small and close ($\Delta_E \simeq e^{-\#V}$), while the energy split for "gapless modes" is slightly larger ($\Delta_E \simeq V^{-\#}$) above topological GSD. Theoretically we can isolate and focus on the effect topologically robust zero modes. Phenomenologically, the degenerate zero modes can contribute low T heat capacity C_V.

[9]However, there is a subtlety that a stronger criterion named the *Haldane null condition* can be used [46]. The condition requires the statistical phase to be strictly zero, $\ell_{a,I} K_{IJ}^{-1} \ell_{a,J} = 0$, instead of just being trivial. In the strict null condition case, we find that $\ell = (2,2)$ is indeed *incompatible* with the coexistence of $\ell = (2,0),(0,2),(2,2)$, see Ref. [30]. The later ℓ vectors have trivial statistics but not null statistics with respect to $\ell = (2,2)$. In the realistic implementation, the stability depends on the relative strength of g couplings.

Our analysis, on GSD with gapped domain walls, closely follows [30] (see also a related work [68]). The periodicity for $\phi_0 \sim \phi_0 + 2\pi$ imposes the quantization of its conjugate variable $P_\phi \in \mathbb{Z}$. Given $[\hat{\phi}_0, \hat{P}_\phi] = i$, the operator relations follow

$$e^{i\hat{P}_\phi \text{m}} |\phi_0\rangle = |\phi_0 - \text{m}\rangle, \quad e^{i\text{n}\hat{\phi}_0} |P_\phi\rangle = |P_\phi + \text{n}\rangle,$$
$$e^{-i\text{n}\hat{\phi}_0} \hat{P}_\phi e^{i\text{n}\hat{\phi}} = \hat{P}_\phi + \text{n}.$$

The $g \cos(\ell_I \cdot \phi_{0I})$ plays two rules: One is the potential pinning down the zero mode ϕ_0 to its minimum, and the other is the hopping term, hopping between the winding mode P_ϕ lattice.

In the zero mode ϕ_0-Hilbert space $\mathcal{H}$, we see that $\mathcal{H} = \{|\phi_{0s},\phi_{0\bar{s}}\rangle\}$ where $(\phi_{0s},\phi_{0\bar{s}}) = (0,0),(\pi,0),(0,\pi),(\pi,\pi)$ mod $(2\pi,2\pi)$, due to the possible presence of all these terms: $\cos(2(\phi_s \pm \phi_{\bar{s}}))$, $\cos(2\phi_s)$, and $\cos(2\phi_{\bar{s}})$ in Eq. (D3). This is shown on the left hand side of Figs. 8(a) and 8(b). In the winding mode P_ϕ-Hilbert space $\mathcal{H}$, we see that $\mathcal{H} = \{|P_{\phi_s}, P_{\phi_{\bar{s}}}\rangle\}$ with both $P_{\phi_I} \in \mathbb{Z}$, thus it forms an integral (two-dimensional) lattice, shown on the right hand side of Figs. 8(a) and 8(b).

How do we compute topological GSD contributed from zero/winding modes? Naively, the minimum of all $(\phi_{0s},\phi_{0\bar{s}})$ contribute different GSD. However, the $\cos(\ell_I \cdot \phi_{0I})$ may be shifted $\cos(\ell_I \cdot \phi_{0I} + \delta)$ by some δ, thus the minimum of $(\phi_{0s},\phi_{0\bar{s}})$ could contain *accidental symmetry breaking* GSD, not the *topological* GSD. Moreover, we should be able to switch the topological sector to different ground states, if we transport the condensed anyons from one edge/domain to the other edge/domain, similar to Laughlin's thought experiment. For example, derived in Ref. [30], by threading background flux $\Delta\Phi_B$ by a unit, the winding mode also jumps a unit, as $q_I \Delta\Phi_B/(\frac{h}{e}) = \Delta P_{\phi,I}$, up to the charge coupling. If we consider a single edge/domain setting, those minimums of zero modes cannot be transported to a different edge, but they contribute GSD naively, thus some of them [in $(0,0)$, $(\pi,0)$, $(0,\pi)$] are accidental or redundant GSD.

To correctly capture the topological GSD, we could better use the winding mode P_ϕ-Hilbert space $\mathcal{H}$. We could project any zero mode basis to winding mode via $\sum_{\substack{P_{\phi_J} = n_a \ell_{a,J}, \\ n_a \in \mathbb{Z},\ \forall a}} |P_{\phi_J}\rangle \cdot \langle P_{\phi_J} | \phi_{0I}\rangle$, and see that the P_{ϕ_J} forms a sublattice of integral lattice; see the right hand side of Figs. 8(a) and 8(b). It is a sublattice with a minimal distance of 2 due to the hopping term from the $\cos(\ell_I \cdot \phi_{0I}) = \frac{(e^{i\ell_I \cdot \phi_{0I}} + e^{-i\ell_I \cdot \phi_{0I}})}{2}$ with a multiple of 2 for ℓ_I in Eq. (D3). Again, on a *single* domain, there is no way to transport the condensed double semions $(s\bar{s})$ to a different domain, the two ways of P_{ϕ_J}-Hilbert space projection in Figs. 8(a) and 8(b) do not imply topological GSD but only a redundancy. However, if we have two edges/domains (say, at Σ_1, Σ_2), there are two robust topological GSD, shown in Fig. 9. There we draw on the left hand side one ground state in $|P_{\phi_s}, \Sigma_1, P_{\phi_{\bar{s}}}, \Sigma_1\rangle \otimes |P_{\phi_s}, \Sigma_2, P_{\phi_{\bar{s}}}, \Sigma_2\rangle$ basis, and the right hand side another ground state in the same basis. The left hand side ground state (up to a choice of projection for a shifting redundancy), however, now can be transported to a different ground state, if we (say, adiabatically) drag one double-semion pair [$s\bar{s}$, that is $\ell' = (1,1)$] from one edge to another edge then condense this $s\bar{s}$. In Fig. 9, this ground state changing from $|\text{gs}_1\rangle$ to $|\text{gs}_2\rangle$ is demonstrated in terms of the dashed arrows. In

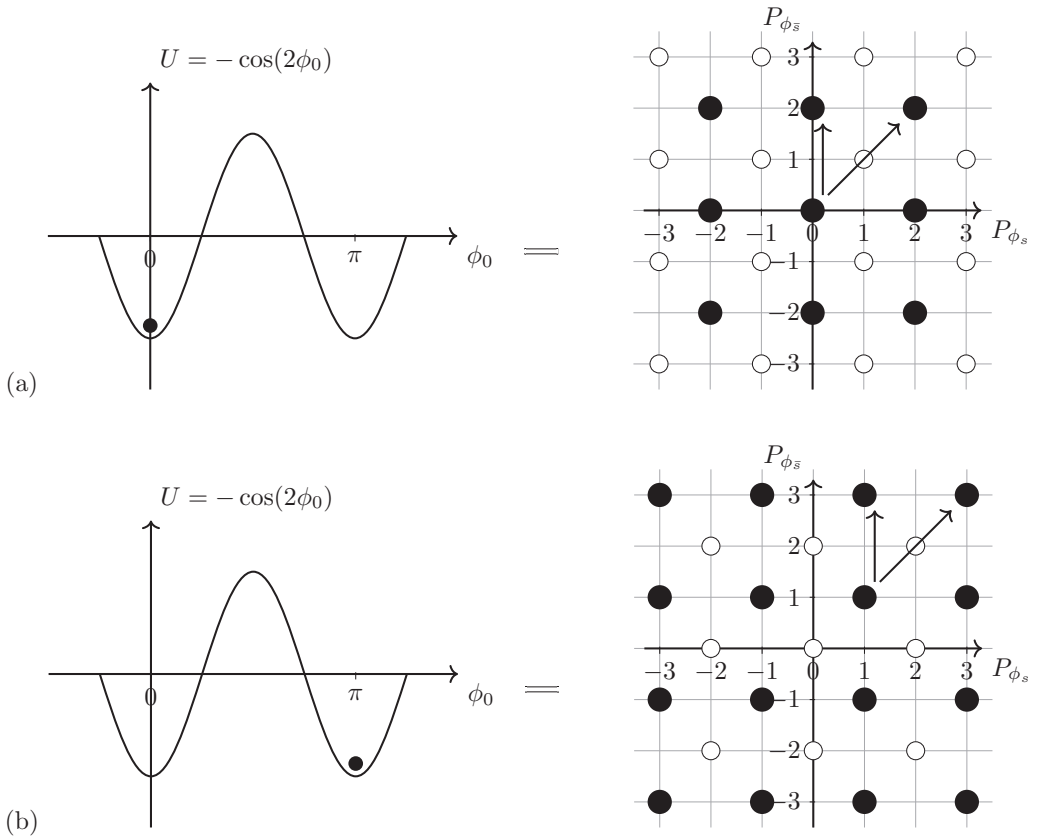

FIG. 8. The left-hand side shows the zero mode ϕ_0-Hilbert space: The ϕ_0 has a 2π periodicity. At the strong coupling cosine term localizes ϕ_0 to 0 and π $\in [0,2\pi)$. Note here $-\cos(2\phi_0)$ and ϕ_0 include a set of allowed potentials $-\cos(2\phi_{0,s}), -\cos(2\phi_{0,\bar{s}})$ and $-\cos(2(\phi_{0,s} \pm \phi_{0,\bar{s}}))$, say in Eq. (D3). The right-hand side shows the winding mode P_{ϕ_s} and $P_{\phi_{\bar{s}}}$-Hilbert space which forms an integral lattice. However, a ground state of localized zero mode $|\phi_{0s},\phi_{0\bar{s}}\rangle$ projected to P_ϕ only forms a sublattice (of unit 2) of the full Hilbert space. The arrows show the hopping from the cosine term $\cos(\ell_I \cdot \phi_{0I})$, shown along the $\ell_I = (2,2)$ and (2,0) directions. In general, the hoppings are allowed in $\ell_I = (2n,2m)$ for $\forall\, n,m \in \mathbb{Z}$. Thus, the black larger disk shows a ground state occupying a sublattice, while the white dot shows another sublattice that can be occupied by another representation of a ground state, in the same P_ϕ-Hilbert space.

this case, $q_I \Delta\Phi_B/(\frac{h}{e}) = (\Delta P_{\phi,s}, \Delta P_{\phi,\bar{s}}) = (1,1)$ say on one edge Σ_1's Hilbert space, but $(\Delta P_{\phi,s}, \Delta P_{\phi,\bar{s}}) = (-1,-1)$ on the other edge Σ_2's Hilbert space. The $|\text{gs}_1\rangle$ and $|\text{gs}_2\rangle$ occupy distinct topological GSD in the Hilbert space. In a field theory view [64], we can say that the topological vacua are tunneled into each other via an extended operator [here the semionic line operator $\int(a_s + a_{\bar{s}})$ in Eq. (B1)] with open ends, ending on two sides of different domain walls. Each end has a pair of double-semions $s\bar{s}$, and there are two pairs of such anyons on two ends. However, when $(\Delta P_{\phi,s}, \Delta P_{\phi,\bar{s}}) = (0,0) \mod 2$, we go back to the same ground state. Namely, transporting even units of $(s\bar{s})$ from one to another domain wall has *no* effect on changing ground states. More generally, we can deduce that for n domain walls, there are additional topological GSD $= 2^{n-1}$ contributed from these zero/winding mode sectors.

APPENDIX E: BOOTSTRAP (NON-)ABELIAN TOPOLOGICAL DOMAIN WALLS

Here we would like to report some analysis of a more general domain wall theory suitable for generic non-Abelian topological orders/TQFT in 2 + 1D, developed in Ref. [61]. This can be viewed as a generalization of Lagrangian subgroup algebra, from Abelian to non-Abelian cases. We like to implement the approach [61] to study the domain walls of non-Abelian Pf|APf quantum Hall states. This will *either* confirm our previous Abelian analysis in Appendix C, or *reveal* something new (which is missed by Abelian Lagrangian subgroup) intrinsically for non-Abelian topological orders.

First, we require the data of topological orders/TQFT, the SL(2,$\mathbb{Z}$) modular representation of $\mathcal{S}^{xy} \equiv \mathcal{S}$ and $\mathcal{T}^{xy} \equiv \mathcal{T}$ matrices, given in Table III. The $\mathcal{S}$ and $\mathcal{T}$ capture the mutual braiding statistics and self exchange statistics (the latter is equivalent to spin statistics), when written in the canonical quasiparticle (anyon) basis. In the canonical basis, we have a diagonal $\mathcal{T}$ matrix such that each entry $\mathcal{T}_{IJ} = \exp(i2\pi s_I)\delta_{IJ}$ tells the spin statistics of anyon labeled by the $\int a_I$ line operator.

1. Nonperturbative bootstrap on topological two-surface defects

Below we implement a nonperturbative bootstrap on topological 1 + 1D domain walls/boundaries of topological orders, based on the method introduced in Ref. [61]. This means that we can bootstrap two-dimensional topological surface defects (two-surface defects), given a 2 + 1D TQFT, for both Abelian and non-Abelian TQFTs. Mathematically, classifying

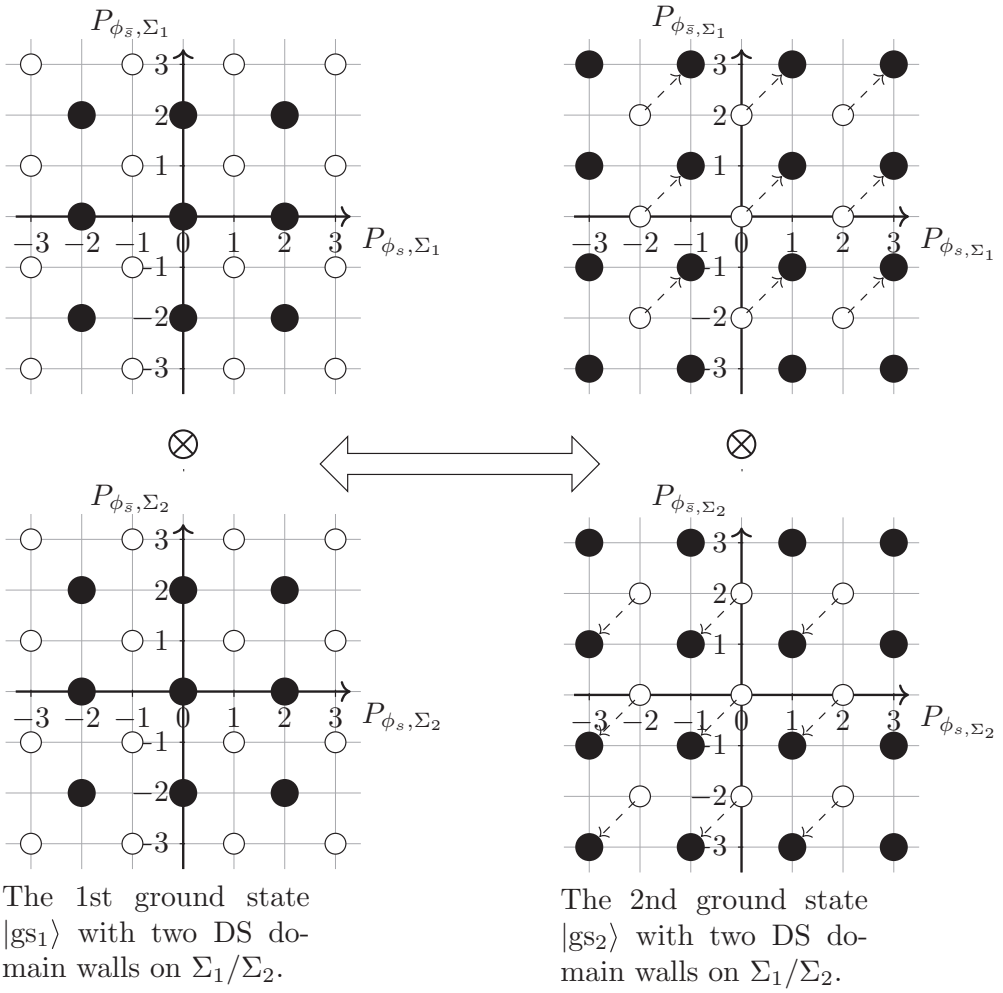

FIG. 9. We illustrate the two ground states, shown in the P_ϕ-Hilbert space, when the quantum state is on a real space with no nontrivial 1-cycle (e.g., flat sample R^2, or S^2) with two gapped double semion (DS) condensed domain walls (Σ_1/Σ_2). The first ground state $|\mathrm{gs}_1\rangle$, on the left side, can be understood as a tensor product ($\otimes$) of two copies of Fig. 8(a) on two edges/domains Σ_1 and Σ_2. The second ground state $|\mathrm{gs}_2\rangle$, on the right side, can be understood as a tensor product ($\otimes$) of two copies of Fig. 8(b) on two edges/domains Σ_1 and Σ_2. The $|\mathrm{gs}_1\rangle$ and $|\mathrm{gs}_2\rangle$ are related by transporting a pair of double semion $s\bar{s}$ from one edge to another edge, causing $(\Delta P_{\phi,s}, \Delta P_{\phi,\bar{s}}) = \ell' = \pm(1,1)$, respectively. This process is shown in terms of dashed arrows.

topological two-surface defects implies a classification of bimodule categories between modular tensor categories (for bosonic TQFTs). Reference [61] labels the topological two-surface defect (1 + 1D topological domain wall) as a *tunneling matrix* $\mathcal{W}$ that we reviewed below.

Given two generic (non-)Abelian TQFTs, say topological orders of A and B, with the data of modular matrices and chiral central charges $\mathcal{S}^A$, $\mathcal{T}^A$, c^A_- and $\mathcal{S}^B$, $\mathcal{T}^B$, c^B_-. Say we have M and N types of line operators (anyons) for TQFT_A and TQFT_B, then, respectively, the rank of modular matrices are M and N. In our treatment, we can first isolate the gapless sector (those chiral sectors cannot be gapped out) away from the possible gappable sectors. If A and B are connected by a gapped two-surface defect, their central charges require to be equal $c^A_- = c^B_-$, at least required for the gappable sector. Reference [61] introduces the domain wall defect labeled by a $N \times M$ *tunneling matrix* $\mathcal{W}$. Each entry $\mathcal{W}_{Ia}$ represents *fusion-space dimensions* within non-negative integers $\mathbb{Z}_{\geqslant 0}$:

$$\mathcal{W}_{Ia} \in \mathbb{Z}_{\geqslant 0}, \tag{E1}$$

satisfying a *commuting criterion* (E2):

$$\mathcal{W}\mathcal{S}^A = \mathcal{S}^B\mathcal{W}, \quad \mathcal{W}\mathcal{T}^A = \mathcal{T}^B\mathcal{W}, \tag{E2}$$

(similar to Lagrangian subgroup, Eq. (E2) imposes the consistency of anyon statistics to condense on a gapped domain wall), and a *stable criterion* (E3):

$$\mathcal{W}_{ia}\mathcal{W}_{jb} \leqslant \sum_{lc} (\mathcal{N}^B)^l_{ij}\mathcal{W}_{lc}(\mathcal{N}^A)^c_{ab}\,. \tag{E3}$$

Here $a,b,c,\ldots / i,j,k,\ldots$ are anyon (line operator) indices for $\mathrm{TQFT}_A/\mathrm{TQFT}_B$. Given modular $\mathcal{S}^A/\mathcal{S}^B$, the fusion rules $(\mathcal{N}^A)^c_{ab}$ and $(\mathcal{N}^B)^k_{ij}$, for $\mathrm{TQFT}_A/\mathrm{TQFT}_B$, are easily determined by Verlinde formula [69], $\mathcal{N}^c_{ab} = \sum_\alpha \frac{\mathcal{S}_{a\alpha}\mathcal{S}_{b\alpha}\mathcal{S}^*_{c\alpha}}{\mathcal{S}_{1\alpha}} \in \mathbb{Z}_{\geqslant 0}$. The criteria whether there exists topological two-surface defect/domain wall, is equivalent to, whether there exists a nonzero solution $\mathcal{W}$ under (E1), (E2), and (E3). (Although additional subtleties can happen, see Reference [61]). We can bootstrap topological two-surface defect/domain wall

between two TQFTs by analytically exhausting all solutions of $\mathcal{W}$.

A tunneling matrix entry $\mathcal{W}_{ia}$ means that the anyon a in TQFT_A has a number of $\mathcal{W}_{ia}$-splitting channels from a to i after going through the domain wall to TQFT_B. Moreover, it is well known that we can use the *folding trick* to relate a gapped domain wall to a gapped boundary. Thus we can bootstrap the topological two-surface defect both in the bulk domain wall and on the boundary.

2. Gapped Pf|APf|Pf domain walls: Curious non-Abelian examples

a. Pf|APf *domain wall*

Now we like to bootstrap various types of topological domain walls at the interface of Pf|APf discussed in Figs. 1, 6, and 7. First we remind the readers that we will focus on the bosonic sectors of Pf/APf quantum Hall states. For bosonic sectors, we recall Table I that Pf quantum Hall state is a semion $\otimes$ Ising topological order [which is a $U(1)_2\times$ Ising TQFT] and APf quantum Hall state is a semion $\otimes SU(2)_{-2}$ topological order [which is a $U(1)_2 \times SU(2)_{-2}$ TQFT]. The Pf|APf interface can be viewed as a domain wall between $U(1)_2\times$ Ising and $U(1)_2 \times SU(2)_{-2}$ TQFTs. By folding trick, we can view it as a boundary of $U(1)_2 \times U(1)_{-2}$ CS $\times$ Ising $\times SU(2)_2$ TQFT to the trivial vacuum, i.e., a boundary of double semions $\times$ Ising $\times SU(2)_2$ TQFT to a vacuum. Since the $c_- = 2$ has four chiral Majorana-Weyl modes on the $1+1$D interface, we find that the bootstrap method in Appendix E 1 for this non-Abelian TQFT actually gives the same result as the Abelian version of Lagrangian subgroup in C. Namely, the sector that can be gapped out is the double-semion theory with K_{DS} in D 1.

b. *Gapped* Pf|APf|Pf *domain walls*

Next we consider the Pf|APf|Pf interface, shown at the corner within the dashed circle of Fig. 1, if the Pf|APf|Pf interface is very closely joined together like a junction.[10] Again by folding trick, we can study the problem in terms of the boundary of $(U(1)_2 \times U(1)_{-2})^2 \times$ Ising $\times \overline{\text{Ising}} \times SU(2)_2 \times SU(2)_{-2}$ TQFT to the trivial vacuum, i.e., a boundary of (double-semions)$^2 \times$ double-Ising $\times$ double-$SU(2)_2$ TQFT to a vacuum. The rank of modular matrices $\mathcal{S}$ and $\mathcal{T}$ for such theory is much higher, as $2^4 \times 3^4 = 1296$. It means that there are 1296 distinct anyons sectors/line operators, and the GSD on T^2-spatial torus is 1296. For simplicity, we can consider that the Abelian sector from $(U(1)_2 \times U(1)_{-2})^2$ CS theory (with 16 anyons), and non-Abelian sector from Ising $\times \overline{\text{Ising}} \times SU(2)_2 \times SU(2)_{-2}$ TQFT (with 81 anyons), separately.

[10]However, we stress that there is a *limitation* of applying the bootstrap method to this example of domain walls in Fig. 1. Ideally, we require that the Pf|APf|Pf interface to be perfectly joined together in a compact circle in a spatial region. But this is not precisely the case in Fig. 1. The applicability of the new Pf|APf|Pf domain wall studied in this section depends on the shared length and the size of the Pf|APf|Pf region, in experimental setups.

Again, the Abelian sector from $(U(1)_2 \times U(1)_{-2})^2$ CS theory can be tackled by the simpler method in Appendix C, gapping by two sets of cosine terms. Moreover, in terms of Appendix E 1's bootstrap method, we can obtain the tunneling data between a double-semion theory and a trivial vacuum as a 4×1 tunneling matrix [61]:

$$\mathcal{W} = \left(\begin{array}{cccc|c} 1 & s & \bar{s} & s\bar{s} & \\ 1 & 0 & 0 & 1 & 1 \end{array}\right). \tag{E4}$$

In this language, we can view a double semion condensation to $s\bar{s}$ to a trivial vacuum after crossing the boundary,

$$1 \oplus s\bar{s} \leftrightarrow 1. \tag{E5}$$

Alternatively, we can also view as the domain wall between two semion theories with this (relatively trivial) tunneling data

$$1 \leftrightarrow 1, \quad s \leftrightarrow s. \tag{E6}$$

The non-Abelian sector from Ising $\times \overline{\text{Ising}} \times SU(2)_2 \times SU(2)_{-2}$ TQFT requires the Appendix E 1's bootstrap method. We can use the folding trick again to consider this problem equivalently as interfaces between Ising $\times SU(2)_2$ TQFT and Ising $\times SU(2)_2$ TQFT (each of them has a set of nine anyons $\{1,\sigma,\psi\} \otimes \{1,\sigma_3,\psi_3\}$). In particular, we find two types of domain wall data, $\mathcal{W}_1$ and $\mathcal{W}_2$:

$$\mathcal{W}_1 = \left(\begin{array}{ccccccccc|c} 1 & \sigma_3 & \psi_3 & \sigma & \sigma\sigma_3 & \sigma\psi_3 & \psi & \psi\sigma_3 & \psi\psi_3 & \\ \hline 1 & 0 & 0 & 0 & 0 & 0 & 0 & 0 & 0 & 1 \\ 0 & 1 & 0 & 0 & 0 & 0 & 0 & 0 & 0 & \sigma_3 \\ 0 & 0 & 1 & 0 & 0 & 0 & 0 & 0 & 0 & \psi_3 \\ 0 & 0 & 0 & 1 & 0 & 0 & 0 & 0 & 0 & \sigma \\ 0 & 0 & 0 & 0 & 1 & 0 & 0 & 0 & 0 & \sigma\sigma_3 \\ 0 & 0 & 0 & 0 & 0 & 1 & 0 & 0 & 0 & \sigma\psi_3 \\ 0 & 0 & 0 & 0 & 0 & 0 & 1 & 0 & 0 & \psi \\ 0 & 0 & 0 & 0 & 0 & 0 & 0 & 1 & 0 & \psi\sigma_3 \\ 0 & 0 & 0 & 0 & 0 & 0 & 0 & 0 & 1 & \psi\psi_3 \end{array}\right), \tag{E7}$$

$$\mathcal{W}_2 = \left(\begin{array}{ccccccccc|c} 1 & \sigma_3 & \psi_3 & \sigma & \sigma\sigma_3 & \sigma\psi_3 & \psi & \psi\sigma_3 & \psi\psi_3 & \\ \hline 1 & 0 & 0 & 0 & 0 & 0 & 0 & 0 & 1 & 1 \\ 0 & 0 & 0 & 0 & 0 & 0 & 0 & 0 & 0 & \sigma_3 \\ 0 & 0 & 1 & 0 & 0 & 0 & 1 & 0 & 0 & \psi_3 \\ 0 & 0 & 0 & 0 & 0 & 0 & 0 & 0 & 0 & \sigma \\ 0 & 0 & 0 & 0 & 2 & 0 & 0 & 0 & 0 & \sigma\sigma_3 \\ 0 & 0 & 0 & 0 & 0 & 0 & 0 & 0 & 0 & \sigma\psi_3 \\ 0 & 0 & 1 & 0 & 0 & 0 & 1 & 0 & 0 & \psi \\ 0 & 0 & 0 & 0 & 0 & 0 & 0 & 0 & 0 & \psi\sigma_3 \\ 1 & 0 & 0 & 0 & 0 & 0 & 0 & 0 & 1 & \psi\psi_3 \end{array}\right). \tag{E8}$$

The $\mathcal{W}_1$ in terms of a 9×9 matrix reveals the tunneling data between two Ising $\times SU(2)_2$ TQFTs:

$$\begin{aligned} &1 \leftrightarrow 1, \quad \sigma_3 \leftrightarrow \sigma_3, \quad \psi_3 \leftrightarrow \psi_3, \\ &\sigma \leftrightarrow \sigma, \quad \sigma\sigma_3 \leftrightarrow \sigma\sigma_3, \quad \sigma\psi_3 \leftrightarrow \sigma\psi_3, \\ &\psi \leftrightarrow \psi, \quad \psi\sigma_3 \leftrightarrow \psi\sigma_3, \quad \psi\psi_3 \leftrightarrow \psi\psi_3. \end{aligned} \tag{E9}$$

Equivalently, if we view $\mathcal{W}_1$ as the boundary to the trivial vacuum, by the folding trick, we can rewrite it as a 81×1 matrix

whose tunneling data is:

$$1 \oplus \sigma\bar{\sigma} \oplus \psi\bar{\psi} \oplus \sigma_3\bar{\sigma}_3 \oplus (\sigma_3\bar{\sigma}_3)(\sigma\bar{\sigma}) \oplus (\sigma_3\bar{\sigma}_3)(\psi\bar{\psi}) \oplus (\psi_3\bar{\psi}_3) \oplus (\psi_3\bar{\psi}_3)(\sigma\bar{\sigma}) \oplus (\psi_3\bar{\psi}_3)(\psi\bar{\psi}) \leftrightarrow 1. \quad \text{(E10)}$$

The $\mathcal{W}_1$ is rather an obvious domain wall in terms of an identity (tunneling) map. However, the $\mathcal{W}_2$ reveals a different but more curious tunneling data between two Ising $\times SU(2)_2$ TQFTs:

$$1 \oplus \psi\psi_3 \leftrightarrow 1 \oplus \psi\psi_3, \quad \psi \oplus \psi_3 \leftrightarrow \psi \oplus \psi_3, \quad 2\sigma\sigma_3 \leftrightarrow 2\sigma\sigma_3. \quad \text{(E11)}$$

In some sense, the domain wall $\mathcal{W}_2$ is more *non-Abelian* than the identity domain wall $\mathcal{W}_1$. We like to capture/contrast their physical properties by computing their GSDs in Appendix E 3.

3. Zero Modes and GSD from (non-)Abelian domain walls

We can compute the topological GSD, here focusing on a flat substrate or a sphere S^2, in the presence of $1+1$D topological domain walls (two-surface defects, studied earlier in Appendix D/E 2) for $2+1$D TQFTs:

(i) For n double-semion [$U(1)_2 \times U(1)_{-2}$ Chern-Simons theory] domain walls, the topological GSD grows as GSD $= 2^{n-1}$.

(ii) For n double-Ising (Ising $\times$ $\overline{\text{Ising}}$ TQFT) domain walls, the topological GSD grows as GSD $= 1,3,10,36,136,\ldots$ for $n = 1,2,3,4,5,\ldots$, which is much faster than 3^{n-1}.

(iii) For n Pf|APf|Pf domain walls of $\mathcal{W}_1$ type, the topological GSD grows as GSD $= 1,9,100,1296,\ldots$ for $n = 1,2,3,4,\ldots$, which is much faster than 8^{n-1}. (Note that the gapped double-semions^2 sectors contribute additional GSD.)

(iv) For n Pf|APf|Pf domain walls of $\mathcal{W}_2$ type, the topological GSD grows as GSD $= 1,12,160,2304,\ldots$ for $n = 1,2,3,4,\ldots$, which is much faster than 12^{n-1}. (Note that the gapped double-semions^2 sectors contribute additional GSD.)

Here are some remarks:

(1) We can derive the general GSD with domain walls, simply given the domain wall tunneling matrix $\mathcal{W}$ and the fusion rule $\mathcal{N}_{ab}^c$, based on generalizing a formula in Ref. [61].

(2) The topological GSD of a given TQFT on a flat substrate or a sphere S^2, in the presence of $0+1$D anyons, can also be computed. In TQFT, this means the path integral Z with n insertions (n punctures) on a sphere, say GSD $= Z(S^2 \times S^1; \sigma_1, \sigma_2, \sigma_3, \ldots)$. This data is fully determined by the fusion rule $\mathcal{N}_{ab}^c$ alone. For instance:

(i) For n semions s (or n double-semions) insertions in the semion (or double-semion) TQFT, the GSD $= 0$ or 1 (i.e., 0 means the configuration is not allowed). This is a signature of an Abelian TQFT.

(ii) For n anyons of $(\sigma\bar{\sigma})$ insertions in double-Ising TQFT, the GSD $= 0,1,0,4,0,16,0,64,\ldots$ for $n = 1,2,3,4,5,6,7,8,\ldots$. The GSD goes as either 0 (not allowed configurations) or 2^{n-2}, where 2 is the quantum dimension of $(\sigma\bar{\sigma})$.

(iii) For any n anyon α insertions in double-Ising $\times$ double-$SU(2)_2$ TQFT, the GSD goes like GSD $\simeq (d_\alpha)^n$ (or no allowed state GSD $= 0$) for large n, bounded by its anyon quantum dimension d_α to the nth power. However, $d_\alpha = 1, \sqrt{2}, 2, 2\sqrt{2}, 4$ for this TQFT. Thus its anyon-insertion GSD $\leqslant 4^n < 10^{n-1} < 12^{n-1}$ grows again much slower than the domain wall $\mathcal{W}_1$ or $\mathcal{W}_2$'s GSD.

In contrast, this GSD caused by anyon insertion grows much *slower* than the *domain wall* GSD. The domain wall GSD for any (non-)Abelian topological orders/TQFT can still have an exponential growth for degenerate states on a sphere S^2 (which is impossible for GSD caused by Abelian anyon insertions alone, by definition of the fusion rule).

(3) Since the domain wall GSD of $\mathcal{W}_2$ grows more rapidly than that of $\mathcal{W}_1$, it suggests that the domain wall $\mathcal{W}_2$ is more *non-Abelian* in nature, in an intriguing way. Detailed investigations on these domain walls are left for the future.

Finally, further intricate domain walls from the joined Abelian and non-Abelian sectors (with a 36×36 anyon tunneling matrix, or by folding trick with a tunneling matrix of 1296 anyons to a trivial sector) for the bosonic TQFT sector of Pf|APf|Pf interface, and also the full fermionic TQFT sector of Pf|APf|Pf interface (e.g., including additional fermionic sector and spin structures for each TQFT), are planned to be studied in the future.

[1] R. Willett, J. P. Eisenstein, H. L. Störmer, D. C. Tsui, A. C. Gossard, and J. H. English, Observation of an Even-Denominator Quantum Number in the Fractional Quantum Hall Effect, Phys. Rev. Lett. **59**, 1776 (1987).

[2] R. H. Morf, Transition from Quantum Hall to Compressible States in the Second Landau Level: New Light on the $\nu = 5/2$ Enigma, Phys. Rev. Lett. **80**, 1505 (1998).

[3] E. H. Rezayi and F. D. M. Haldane, Incompressible Paired Hall State, Stripe Order, and the Composite Fermion Liquid Phase in Half-Filled Landau Levels, Phys. Rev. Lett. **84**, 4685 (2000).

[4] M. R. Peterson, T. Jolicoeur, and S. Das Sarma, Finite-Layer Thickness Stabilizes the Pfaffian State for the 5/2 Fractional Quantum Hall Effect: Wave Function Overlap and Topological Degeneracy, Phys. Rev. Lett. **101**, 016807 (2008).

[5] A. E. Feiguin, E. Rezayi, K. Yang, C. Nayak, and S. Das Sarma, Spin polarization of the $\nu = 5/2$ quantum Hall state, Phys. Rev. B **79**, 115322 (2009).

[6] H. Wang, D. N. Sheng, and F. D. M. Haldane, Particle-hole symmetry breaking and the $\nu = \frac{5}{2}$ fractional quantum Hall effect, Phys. Rev. B **80**, 241311 (2009).

[7] M. Storni, R. H. Morf, and S. Das Sarma, Fractional Quantum Hall State at $\nu = \frac{5}{2}$ and the Moore-Read Pfaffian, Phys. Rev. Lett. **104**, 076803 (2010).

[8] E. H. Rezayi and S. H. Simon, Breaking of Particle-Hole Symmetry by Landau Level Mixing in the $\nu = 5/2$ Quantized Hall State, Phys. Rev. Lett. **106**, 116801 (2011).

[9] Z. Papić, F. D. M. Haldane, and E. H. Rezayi, Quantum Phase Transitions and the $\nu = 5/2$ Fractional Hall State in Wide Quantum Wells, Phys. Rev. Lett. **109**, 266806 (2012).

[10] M. P. Zaletel, R. S. K. Mong, F. Pollmann, and E. H. Rezayi, Infinite density matrix renormalization group for multicomponent quantum Hall systems, Phys. Rev. B **91**, 045115 (2015).

[11] K. Pakrouski, M. R. Peterson, T. Jolicoeur, V. W. Scarola, C. Nayak, and M. Troyer, Phase Diagram of the $\nu = 5/2$ Fractional Quantum Hall Effect: Effects of Landau-Level Mixing and Nonzero Width, Phys. Rev. X **5**, 021004 (2015).

[12] G. Moore and N. Read, Nonabelions in the fractional quantum Hall effect, Nucl. Phys. B **360**, 362 (1991).

[13] N. Read and D. Green, Paired states of fermions in two dimensions with breaking of parity and time-reversal symmetries and the fractional quantum Hall effect, Phys. Rev. B **61**, 10267 (2000).

[14] M. Levin, B. I. Halperin, and B. Rosenow, Particle-Hole Symmetry and the Pfaffian State, Phys. Rev. Lett. **99**, 236806 (2007).

[15] S.-S. Lee, S. Ryu, C. Nayak, and M. P. A. Fisher, Particle-Hole Symmetry and the $\nu = \frac{5}{2}$ Quantum Hall State, Phys. Rev. Lett. **99**, 236807 (2007).

[16] X. G. Wen, Non-Abelian Statistics in the Fractional Quantum Hall States, Phys. Rev. Lett. **66**, 802 (1991).

[17] C. L. Kane and M. P. A. Fisher, Quantized thermal transport in the fractional quantum Hall effect, Phys. Rev. B **55**, 15832 (1997).

[18] X.-G. Wen, Topological Order and Edge Structure of $\nu = 1/2$ Quantum Hall State, Phys. Rev. Lett. **70**, 355 (1993).

[19] M. Banerjee, M. Heiblum, V. Umansky, D. E. Feldman, Y. Oreg, and A. Stern, Observation of half-integer thermal Hall conductance, arXiv:1710.00492.

[20] P. T. Zucker and D. E. Feldman, Stabilization of the Particle-Hole Pfaffian Order by Landau-Level Mixing and Impurities that Break Particle-Hole Symmetry, Phys. Rev. Lett. **117**, 096802 (2016).

[21] D. T. Son, Is the Composite Fermion a Dirac Particle? Phys. Rev. X **5**, 031027 (2015).

[22] X. Chen, L. Fidkowski, and A. Vishwanath, Symmetry enforced non-Abelian topological order at the surface of a topological insulator, Phys. Rev. B **89**, 165132 (2014).

[23] C. Wang, A. Vishwanath, and B. I. Halperin, Topological order from disorder and the quantized Hall thermal metal: Possible applications to the $\nu = \frac{5}{2}$ state, arXiv:1711.11557.

[24] D. F. Mross, Y. Oreg, A. Stern, G. Margalit, and M. Heiblum, Theory of disorder-induced half-integer thermal Hall conductance, arXiv:1711.06278.

[25] T. Senthil and M. P. A. Fisher, Quasiparticle localization in superconductors with spin-orbit scattering, Phys. Rev. B **61**, 9690 (2000).

[26] J. T. Chalker, N. Read, V. Kagalovsky, B. Horovitz, Y. Avishai, and A. W. W. Ludwig, Thermal metal in network models of a disordered two-dimensional superconductor, Phys. Rev. B **65**, 012506 (2001).

[27] I. C. Fulga, A. R. Akhmerov, J. Tworzydło, B. Béri, and C. W. J. Beenakker, Thermal metal-insulator transition in a helical topological superconductor, Phys. Rev. B **86**, 054505 (2012).

[28] Y. Imry and S.-K. Ma, Random-Field Instability of the Ordered State of Continuous Symmetry, Phys. Rev. Lett. **35**, 1399 (1975).

[29] K. Binder, Random-field induced interface widths in Ising systems, Z. Phys. B **50**, 343 (1983).

[30] J. C. Wang and X.-G. Wen, Boundary degeneracy of topological order, Phys. Rev. B **91**, 125124 (2015).

[31] M. Levin, Protected Edge Modes Without Symmetry, Phys. Rev. X **3**, 021009 (2013).

[32] N. Read and E. Rezayi, Quasiholes and fermionic zero modes of paired fractional quantum Hall states: The mechanism for non-Abelian statistics, Phys. Rev. B **54**, 16864 (1996).

[33] M. Milovanović and N. Read, Edge excitations of paired fractional quantum Hall states, Phys. Rev. B **53**, 13559 (1996).

[34] S. M. Girvin, Particle-hole symmetry in the anomalous quantum Hall effect, Phys. Rev. B **29**, 6012 (1984).

[35] B. I. Halperin, P. A. Lee, and N. Read, Theory of the half-filled Landau level, Phys. Rev. B **47**, 7312 (1993).

[36] J. K. Jain, Composite-Fermion Approach for the Fractional Quantum Hall Effect, Phys. Rev. Lett. **63**, 199 (1989).

[37] D. F. Mross, A. Essin, and J. Alicea, Composite Dirac Liquids: Parent States for Symmetric Surface Topological Order, Phys. Rev. X **5**, 011011 (2015).

[38] S. D. Geraedts, M. P. Zaletel, R. S. K. Mong, M. A. Metlitski, A. Vishwanath, and O. I. Motrunich, The half-filled Landau level: The case for dirac composite fermions, Science **352**, 197 (2016).

[39] C. Wang and T. Senthil, Composite Fermi liquids in the lowest Landau level, Phys. Rev. B **94**, 245107 (2016).

[40] A. C. Potter, M. Serbyn, and A. Vishwanath, Thermoelectric Transport Signatures of Dirac Composite Fermions in the Half-Filled Landau Level, Phys. Rev. X **6**, 031026 (2016).

[41] S. D. Geraedts, J. Wang, E. Rezayi, and F. D. M. Haldane, Berry phase and model wavefunction in the half-filled Landau level, arXiv:1711.07864.

[42] J. T. Chalker and P. D. Coddington, Percolation, quantum tunneling and the integer hall effect, J. Phys. C **21**, 2665 (1988).

[43] B. Kramer, T. Ohtsuki, and S. Kettemann, Random network models and quantum phase transitions in two dimensions, Phys. Rep. **417**, 211 (2005).

[44] A. Altland and M. R. Zirnbauer, Nonstandard symmetry classes in mesoscopic normal-superconducting hybrid structures, Phys. Rev. B **55**, 1142 (1997).

[45] C. L. Kane, M. P. A. Fisher, and J. Polchinski, Randomness at the Edge: Theory of Quantum Hall Transport at Filling $\nu = 2/3$, Phys. Rev. Lett. **72**, 4129 (1994).

[46] F. D. M. Haldane, Stability of Chiral Luttinger Liquids and Abelian Quantum Hall States, Phys. Rev. Lett. **74**, 2090 (1995).

[47] X. Wan, A. M. Turner, A. Vishwanath, and S. Y. Savrasov, Topological semimetal and Fermi-arc surface states in the electronic structure of pyrochlore iridates, Phys. Rev. B **83**, 205101 (2011).

[48] L. Balents, Weyl electrons kiss, Physics **4**, 36 (2011).

[49] A. M. M. Pruisken, Universal Singularities in the Integral Quantum Hall Effect, Phys. Rev. Lett. **61**, 1297 (1988).

[50] J. Wang, B. Lian, and S.-C. Zhang, Universal scaling of the quantum anomalous Hall plateau transition, Phys. Rev. B **89**, 085106 (2014).

[51] Q. L. He, L. Pan, A. L. Stern, E. C. Burks, X. Che, G. Yin *et al.*, Chiral majorana fermion modes in a quantum anomalous hall insulator–superconductor structure, Science **357**, 294 (2017).

[52] B. Lian, J. Wang, X.-Q. Sun, A. Vaezi, and S.-C. Zhang, Quantum phase transition of chiral Majorana fermions in the presence of disorder, Phys. Rev. B **97**, 125408 (2018).

[53] J. M. Luttinger, Fermi surface and some simple equilibrium properties of a system of interacting fermions, Phys. Rev. **119**, 1153 (1960).

[54] A. C. Balram, C. Tőke, and J. K. Jain, Luttinger Theorem for the Strongly Correlated Fermi Liquid of Composite Fermions, Phys. Rev. Lett. **115**, 186805 (2015).

[55] V. L. Berezinskii, Destruction of long-range order in one-dimensional and two-dimensional systems having a continuous symmetry group I. classical systems, Zh. Eksp. Teor. Fiz. **59**, 907 (1970) [Sov. Phys. JETP **32**, 493 (1971)].

[56] J. M. Kosterlitz and D. J. Thouless, Ordering, metastability and phase transitions in two-dimensional systems, J. Phys. C **6**, 1181 (1973).

[57] G. Yang and D. E. Feldman, Influence of device geometry on tunneling in the $\nu = \frac{5}{2}$ quantum Hall liquid, Phys. Rev. B **88**, 085317 (2013).

[58] M. Barkeshli, M. Mulligan, and M. P. A. Fisher, Particle-hole symmetry and the composite Fermi liquid, Phys. Rev. B **92**, 165125 (2015).

[59] X. Wan and K. Yang, Striped quantum Hall state in a half-filled Landau level, Phys. Rev. B **93**, 201303 (2016).

[60] T. Iadecola, T. Neupert, C. Chamon, and C. Mudry, Accessing topological order in fractionalized liquids with gapped edges, Phys. Rev. B **90**, 205115 (2014).

[61] T. Lan, J. C. Wang, and X.-G. Wen, Gapped Domain Walls, Gapped Boundaries, and Topological Degeneracy, Phys. Rev. Lett. **114**, 076402 (2015).

[62] N. Seiberg and E. Witten, Gapped boundary phases of topological insulators via weak coupling, Prog. Theor. Exper. Phys. **2016**, 12C101 (2016).

[63] P. Putrov, J. Wang, and S.-T. Yau, Braiding statistics and link invariants of bosonic/fermionic topological quantum matter in 2+1 and 3+1 dimensions, Ann. Phys. **384**, 254 (2017).

[64] J. Wang, K. Ohmori, P. Putrov, Y. Zheng, Z. Wan, M. Guo, H. Lin, P. Gao, and S. T. Yau, Tunneling Topological Vacua via Extended Operators: (Spin-)TQFT Spectra and Boundary Deconfinement in Various Dimensions, arXiv:1801.05416.

[65] A. Kitaev, Anyons in an exactly solved model and beyond, Ann. Phys. **321**, 2 (2006).

[66] G. Moore and N. Seiberg, Classical and quantum conformal field theory, Commun. Math. Phys. **123**, 177 (1989).

[67] A. Kapustin and N. Saulina, Topological boundary conditions in Abelian Chern-Simons theory, Nucl. Phys. B **845**, 393 (2011).

[68] A. Kapustin, Ground-state degeneracy for Abelian anyons in the presence of gapped boundaries, Phys. Rev. B **89**, 125307 (2014).

[69] E. P. Verlinde, Fusion rules and modular transformations in 2D conformal field theory, Nucl. Phys. B **300**, 360 (1988).